to compensatory mechanisms for endochondral ossification, such as an increase of proteinases other than MMP9. In fact, proteinases, such as MMP13, tended to be regulated oppositely to MMP9 by the KLF5 overexpression (Fig. 3*B* and Table 1). Since MMPs are known to play roles under various pathological conditions, including wound healing, arthritis, and tumor development (45–47), we examined the effects of KLF5 insufficiency on bone fracture and arthritis by making the models in KLF5$^{+/-}$ mice at 8 weeks of age (supplemental Fig. 5, *A* and *B*). In results, there was no difference in fracture healing or arthritis development between KLF5$^{+/-}$ and the wild-type littermates. KLF5 may therefore be indispensable for skeletal development only in the perinatal period but be dispensable after birth under physiological and pathological conditions. Another possible compensatory mechanism is bone formation by osteoblasts, despite the expression of KLF5 in the cells (Fig. 1). This osteoblastic compensation may be sufficient to make up for the KLF5 dysfunction in chondrocytes after a substantial number of osteoblasts have appeared after birth but insufficient in the perinatal period when chondrocytes play central roles in endochondral ossification. Generation and evaluation of conditional knockout mice will clarify the tissue-specific roles of KLF5. In addition, further understanding of the molecular network related to the KLF5-MMP9 axis will greatly help us to unravel the complex mechanism modulating endochondral ossification.

REFERENCES

1. Kronenberg, H. M. (2003) *Nature* **423,** 332–336
2. Karsenty, G., and Wagner, E. F. (2002) *Dev. Cell* **2,** 389–406
3. Vu, T. H., Shipley, J. M., Bergers, G., Berger, J. E., Helms, J. A., Hanahan, D., Shapiro, S. D., Senior, R. M., and Werb, Z. (1998) *Cell* **93,** 411–422
4. Ortega, N., Behonick, D., Stickens, D., and Werb, Z. (2003) *Ann. N. Y. Acad. Sci.* **995,** 109–116
5. Stickens, D., Behonick, D. J., Ortega, N., Heyer, B., Hartenstein, B., Yu, Y., Fosang, A. J., Schorpp-Kistner, M., Angel, P., and Werb, Z. (2004) *Development* **131,** 5883–5895
6. Inada, M., Wang, Y., Byrne, M. H., Rahman, M. U., Miyaura, C., Lopez-Otin, C., and Krane, S. M. (2004) *Proc. Natl. Acad. Sci. U. S. A.* **101,** 17192–17197
7. Lee, E. R., Murphy, G., El-Alfy, M., Davoli, M. A., Lamplugh, L., Docherty, A. J., and Leblond, C. P. (1999) *Dev. Dyn.* **215,** 190–205
8. Werb, Z. (1997) *Cell* **91,** 439–442
9. Kaczynski, J., Cook, T., and Urrutia, R. (2003) *Genome Biol.* **4,** 206
10. van Vliet, J., Crofts, L. A., Quinlan, K. G., Czolij, R., Perkins, A. C., and Crossley, M. (2006) *Genomics* **87,** 474–482
11. Bieker, J. J. (2001) *J. Biol. Chem.* **276,** 34355–34358
12. Watanabe, N., Kurabayashi, M., Shimomura, Y., Kawai-Kowase, K., Hoshino, Y., Manabe, I., Watanabe, M., Aikawa, M., Kuro-o, M., Suzuki, T., Yazaki, Y., and Nagai, R. (1999) *Circ. Res.* **85,** 182–191
13. Ohnishi, S., Laub, F., Matsumoto, N., Asaka, M., Ramirez, F., Yoshida, T., and Terada, M. (2000) *Dev. Dyn.* **217,** 421–429
14. Conkright, M. D., Wani, M. A., Anderson, K. P., and Lingrel, J. B (1999) *Nucleic Acids Res.* **27,** 1263–1270
15. Shindo, T., Manabe, I., Fukushima, Y., Tobe, K., Aizawa, K., Miyamoto, S., Kawai-Kowase, K., Moriyama, N., Imai, Y., Kawakami, H., Nishimatsu, H., Ishikawa, T., Suzuki, T., Morita, H., Maemura, K., Sata, M., Hirata, Y., Komukai, M., Kagechika, H., Kadowaki, T., Kurabayashi, M., and Nagai, R. (2002) *Nat. Med.* **8,** 856–863
16. Oishi, Y., Manabe, I., Tobe, K., Tsushima, K., Shindo, T., Fujiu, K., Nishimura, G., Maemura, K., Yamauchi, T., Kubota, N., Suzuki, R., Kitamura, T., Akira, S., Kadowaki, T., and Nagai, R. (2005) *Cell Metab.* **1,** 27–39
17. Gollner, H., Dani, C., Phillips, B., Philipsen, S., and Suske, G. (2001) *Mech. Dev.* **106,** 77–83
18. Nakashima, K., Zhou, X., Kunkel, G., Zhang, Z., Deng, J. M., Behringer, R. R., and de Crombrugghe, B. (2002) *Cell* **108,** 17–29
19. Lefebvre, V., Garofalo, S., Zhou, G., Metsaranta, M., Vuorio, E., and De Crombrugghe, B. (1994) *Matrix Biol.* **14,** 329–335
20. Kobayashi, K., Takahashi, N., Jimi, E., Udagawa, N., Takami, M., Kotake, S., Nakagawa, N., Kinosaki, M., Yamaguchi, K., Shima, N., Yasuda, H., Morinaga, T., Higashio, K., Martin, T. J., and Suda, T. (2000) *J. Exp. Med.* **191,** 275–286
21. Aizawa, K., Suzuki, T., Kada, N., Ishihara, A., Kawai-Kowase, K., Matsumura, T., Sasaki, K., Munemasa, Y., Manabe, I., Kurabayashi, M., Collins, T., and Nagai, R. (2004) *J. Biol. Chem.* **279,** 70–76
22. Shimoaka, T., Kamekura, S., Chikuda, H., Hoshi, K., Chung, U. I., Akune, T., Maruyama, Z., Komori, T., Matsumoto, M., Ogawa, W., Terauchi, Y., Kadowaki, T., Nakamura, K., and Kawaguchi, H. (2004) *J. Biol. Chem.* **279,** 15314–15322
23. Yamada, T., Kawano, H., Koshizuka, Y., Fukuda, T., Yoshimura, K., Kamekura, S., Saito, T., Ikeda, T., Kawasaki, Y., Azuma, Y., Ikegawa, S., Hoshi, K., Chung, U. I., Nakamura, K., Kato, S., and Kawaguchi, H. (2006) *Nat. Med.* **12,** 665–670
24. Terato, K., Harper, D. S., Griffiths, M. M., Hasty, D. L., Ye, X. J., Cremer, M. A., and Seyer, J. M. (1995) *Autoimmunity* **22,** 137–147
25. Terato, K., Hasty, K. A., Reife, R. A., Cremer, M. A., Kang, A. H., and Stuart, J. M. (1992) *J. Immunol.* **148,** 2103–2108
26. Reponen, P., Sahlberg, C., Munaut, C., Thesleff, I., and Tryggvason, K. (1994) *Ann. N. Y. Acad. Sci.* **732,** 472–475
27. Engsig, M. T., Chen, Q. J., Vu, T. H., Pedersen, A. C., Therkidsen, B., Lund, L. R., Henriksen, K., Lenhard, T., Foged, N. T., Werb, Z., and Delaisse, J. M. (2000) *J. Cell Biol.* **151,** 879–889
28. Perez-Moreno, M., and Fuchs, E. (2006) *Dev. Cell* **11,** 601–612
29. Torres, M., Stoykova, A., Huber, O., Chowdhury, K., Bonaldo, P., Mansouri, A., Butz, S., Kemler, R., and Gruss, P. (1997) *Proc. Natl. Acad. Sci. U. S. A.* **94,** 901–906
30. Kobielak, A., and Fuchs, E. (2006) *Proc. Natl. Acad. Sci. U. S. A.* **103,** 2322–2327
31. Tortorella, M. D., Burn, T. C., Pratta, M. A., Abbaszade, I., Hollis, J. M., Liu, R., Rosenfeld, S. A., Copeland, R. A., Decicco, C. P., Wynn, R., Rockwell, A., Yang, F., Duke, J. L., Solomon, K., George, H., Bruckner, R., Nagase, H., Itoh, Y., Ellis, D. M., Ross, H., Wiswall, B. H., Murphy, K., Hillman, M. C., Jr., Hollis, G. F., Newton, R. C., Magolda, R. L., Trzaskos, J. M., and Arner, E. C. (1999) *Science* **284,** 1664–1666
32. Pratta, M. A., Yao, W., Decicco, C., Tortorella, M. D., Liu, R. Q., Copeland, R. A., Magolda, R., Newton, R. C., Trzaskos, J. M., and Arner, E. C. (2003) *J. Biol. Chem.* **278,** 45539–45545
33. Holmbeck, K., Bianco, P., Caterina, J., Yamada, S., Kromer, M., Kuznetsov, S. A., Mankani, M., Robey, P. G., Poole, A. R., Pidoux, I., Ward, J. M., and Birkedal-Hansen, H. (1999) *Cell* **99,** 81–92
34. Zhou, Z., Apte, S. S., Soininen, R., Cao, R., Baaklini, G. Y., Rauser, R. W., Wang, J., Cao, Y., and Tryggvason, K. (2000) *Proc. Natl. Acad. Sci. U. S. A.* **97,** 4052–4057
35. Haeusler, G., Walter, I., Helmreich, M., and Egerbacher, M. (2005) *Calcif. Tissue Int.* **76,** 326–335
36. Colnot, C., Sidhu, S. S., Balmain, N., and Poirier, F. (2001) *Dev. Biol.* **229,** 203–214
37. Gerber, H. P., Vu, T. H., Ryan, A. M., Kowalski, J., Werb, Z., and Ferrara, N. (1999) *Nat. Med.* **5,** 623–628
38. Maes, C., Carmeliet, P., Moermans, K., Stockmans, I., Smets, N., Collen, D., Bouillon, R., and Carmeliet, G. (2002) *Mech. Dev.* **111,** 61–73
39. Zelzer, E., Mamluk, R., Ferrara, N., Johnson, R. S., Schipani, E., and Olsen, B. R. (2004) *Development* **131,** 2161–2171
40. Zelzer, E., McLean, W., Ng, Y. S., Fukai, N., Reginato, A. M., Lovejoy, S., D'Amore, P. A., and Olsen, B. R. (2002) *Development* **129,** 1893–1904
41. Bluteau, G., Julien, M., Magne, D., Mallein-Gerin, F., Weiss, P., Daculsi, G., and Guicheux, J. (2007) *Bone* **40,** 568–576
42. Naldini, L., Vigna, E., Bardelli, A., Follenzi, A., Galimi, F., and Comoglio, P. M. (1995) *J. Biol. Chem.* **270,** 603–611

43. Jingushi, S., Scully, S. P., Joyce, M. E., Sugioka, Y., and Bolander, M. E. (1995) *J. Orthop. Res.* **13,** 761–768
44. Whitelock, J. M., Murdoch, A. D., Iozzo, R. V., and Underwood, P. A. (1996) *J. Biol. Chem.* **271,** 10079–10086
45. Milner, J. M., and Cawston, T. E. (2005) *Curr. Drug Targets Inflamm. Allergy* **4,** 363–375
46. Colnot, C., Thompson, Z., Miclau, T., Werb, Z., and Helms, J. A. (2003) *Development* **130,** 4123–4133
47. Kosaki, N., Takaishi, H., Kamekura, S., Kimura, T., Okada, Y., Minqi, L., Amizuka, N., Chung, U. I., Nakamura, K., Kawaguchi, H., Toyama, Y., and D'Armiento, J. (2007) *Biochem. Biophys. Res. Commun.* **354,** 846–851

Phosphorylation of GSK-3β by cGMP-dependent protein kinase II promotes hypertrophic differentiation of murine chondrocytes

Yosuke Kawasaki,[1] Fumitaka Kugimiya,[1] Hirotaka Chikuda,[1] Satoru Kamekura,[1] Toshiyuki Ikeda,[1] Naohiro Kawamura,[1] Taku Saito,[1] Yusuke Shinoda,[1] Akiro Higashikawa,[1] Fumiko Yano,[1] Toru Ogasawara,[1] Naoshi Ogata,[1] Kazuto Hoshi,[1] Franz Hofmann,[2] James R. Woodgett,[3] Kozo Nakamura,[1] Ung-il Chung,[1] and Hiroshi Kawaguchi[1]

[1]Sensory and Motor System Medicine, Faculty of Medicine, University of Tokyo, Tokyo, Japan. [2]Institut für Pharmakologie und Toxikologie, Technische Universität München, Munich, Germany. [3]Samuel Lunenfeld Research Institute, Toronto, Ontario, Canada.

cGMP-dependent protein kinase II (cGKII; encoded by *PRKG2*) is a serine/threonine kinase that is critical for skeletal growth in mammals; in mice, cGKII deficiency results in dwarfism. Using radiographic analysis, we determined that this growth defect was a consequence of an elongated growth plate and impaired chondrocyte hypertrophy. To investigate the mechanism of cGKII-mediated chondrocyte hypertrophy, we performed a kinase substrate array and identified glycogen synthase kinase–3β (GSK-3β; encoded by *Gsk3b*) as a principal phosphorylation target of cGKII. In cultured mouse chondrocytes, phosphorylation-mediated inhibition of GSK-3β was associated with enhanced hypertrophic differentiation. Furthermore, cGKII induction of chondrocyte hypertrophy was suppressed by cotransfection with a phosphorylation-deficient mutant of GSK-3β. Analyses of mice with compound deficiencies in both protein kinases (*Prkg2*$^{-/-}$*Gsk3b*$^{+/-}$) demonstrated that the growth retardation and elongated growth plate associated with cGKII deficiency were partially rescued by haploinsufficiency of *Gsk3b*. We found that β-catenin levels decreased in *Prkg2*$^{-/-}$ mice, while overexpression of cGKII increased the accumulation and transactivation function of β-catenin in mouse chondroprogenitor ATDC5 cells. This effect was blocked by coexpression of phosphorylation-deficient GSK-3β. These data indicate that hypertrophic differentiation of growth plate chondrocytes during skeletal growth is promoted by phosphorylation and inactivation of GSK-3β by cGKII.

Introduction

Skeletal growth is achieved by endochondral ossification in the growth plate cartilage, with orderly columnar arrays of resting, proliferative, and hypertrophic zones of chondrocytes. During the process, chondrocytes undergo proliferation, hypertrophic differentiation, and apoptosis, each of which is regulated by distinct molecular signaling systems (1). Among them, C-type natriuretic peptide (CNP; encoded by *Nppc*), a humoral factor that can regulate a variety of homeostatic processes by binding the membrane-bound guanylyl cyclase–coupled receptor B (GC-B; encoded by *Npr2*), has been shown to play important roles in skeletal growth, because mice deficient in either gene exhibit impaired skeletal growth (2, 3). Loss-of-function mutations in *Npr2* also show dwarfism in patients known as acromesomelic dysplasia, type Maroteaux (4), demonstrating the importance of CNP/GC-B signaling in the skeletal growth of humans as well. This signaling causes the intracellular accumulation of cGMP, which then activates cGMP-dependent protein kinases (cGKs) (5). In mammalian cells, there are 2 cGK isoforms, cGKI and cGKII (encoded by *Prkg1* and *Prkg2*, respectively), which show distinct distributions and functions (6, 7). Although both are expressed in growth plate cartilage, *Prkg2*$^{-/-}$ mice show postnatal dwarfism with about 20%–30% reduction in the length of limbs and trunk (6), while *Prkg1*$^{-/-}$ mice show a normal skeleton (8), indicating that only cGKII is indispensable for skeletal growth.

cGKII is a membrane-bound serine/threonine kinase with a cGMP-binding domain and a catalytic domain in the C terminus (7). In addition to growth retardation resulting from cGKII deficiency in mice, our previous positional cloning analysis identified a deletion in *Prkg2*, the rat gene encoding cGKII, in the Komeda miniature rat Ishikawa (KMI), a naturally occurring mutant rat, which also exhibited dwarfism with 20%–30% shorter long bones and vertebrae (9). The deletion resulted in a frame shift and a premature stop codon, predicting a truncated cGKII protein that lacks the kinase domain (cGKII-Δkinase). KMI rats show an elongated growth plate, whose height is about 2.5-fold that of WT littermates. This is caused by the existence of an abnormal intermediate layer between the proliferative and hypertrophic zones with accumulation of few proliferative or hypertrophic chondrocytes, which indicates that the kinase activity of cGKII is necessary for

Nonstandard abbreviations used: ALP, alkaline phosphatase; Bad, BCL2-antagonist of cell death; cdc25, cell division cycle 25 homolog; cGK, cGMP-dependent protein kinase; cGKII-Δkinase, truncated cGKII protein that lacks the kinase domain; CNP, C-type natriuretic peptide; COL10, type X collagen; GC-B, guanylyl cyclase–coupled receptor B; GSK-3β, glycogen synthase kinase–3β; GSK-3β^{S9A}, phosphorylation-deficient mutant of GSK-3β with a serine-to-alanine substitution; PLK, polo-like kinase; p90RSK, 90-kDa ribosomal protein S6 kinase; PTH, parathyroid hormone; PTHrP, parathyroid hormone–related protein; TCF, T cell factor; VASP, vasodilator-stimulated phosphoprotein.

Conflict of interest: The authors have declared that no conflict of interest exists.

Citation for this article: *J. Clin. Invest.* **118**:2506–2515 (2008). doi:10.1172/JCI35243.

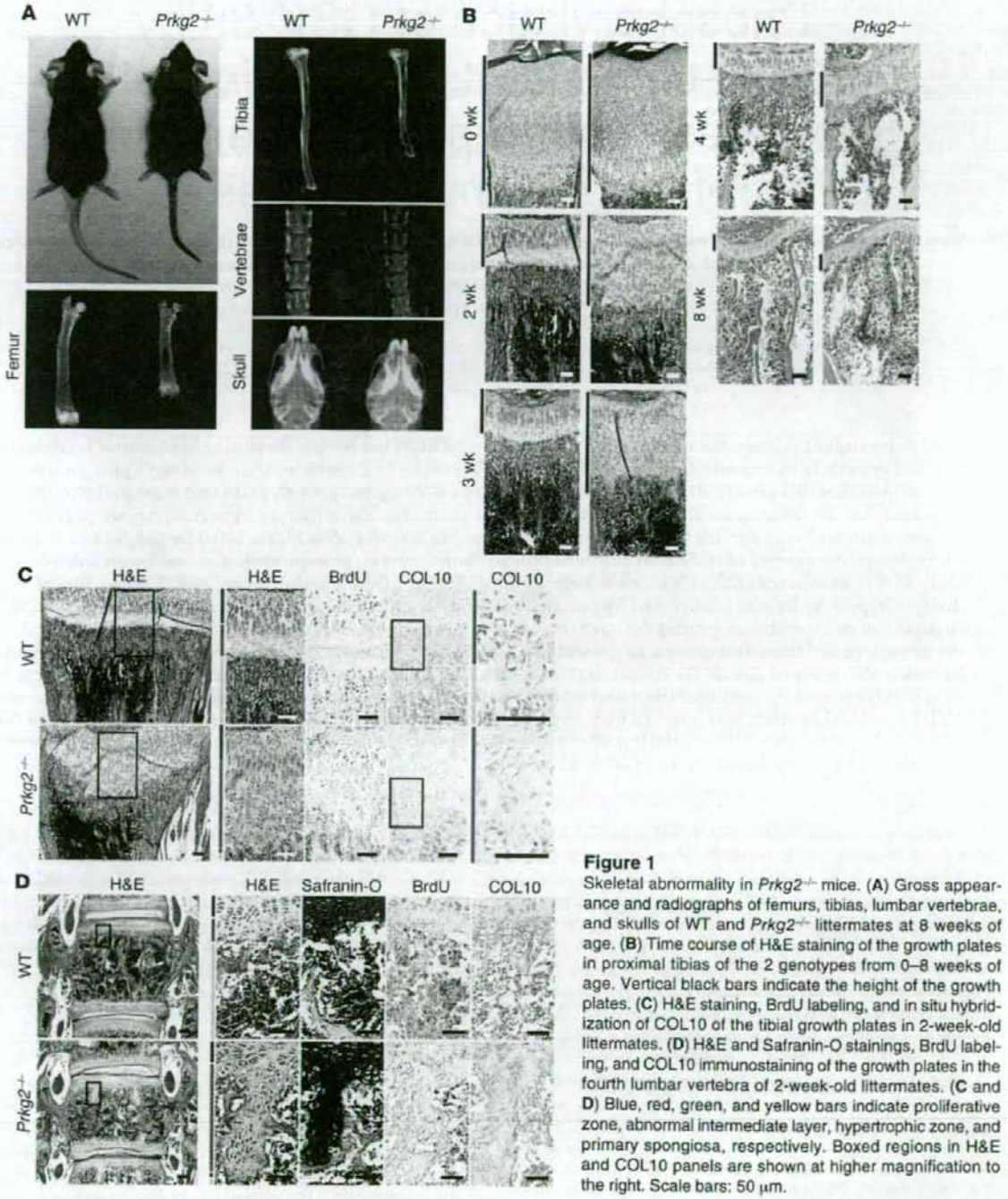

Figure 1

Skeletal abnormality in *Prkg2*$^{-/-}$ mice. (**A**) Gross appearance and radiographs of femurs, tibias, lumbar vertebrae, and skulls of WT and *Prkg2*$^{-/-}$ littermates at 8 weeks of age. (**B**) Time course of H&E staining of the growth plates in proximal tibias of the 2 genotypes from 0–8 weeks of age. Vertical black bars indicate the height of the growth plates. (**C**) H&E staining, BrdU labeling, and in situ hybridization of COL10 of the tibial growth plates in 2-week-old littermates. (**D**) H&E and Safranin-O stainings, BrdU labeling, and COL10 immunostaining of the growth plates in the fourth lumbar vertebra of 2-week-old littermates. (**C** and **D**) Blue, red, green, and yellow bars indicate proliferative zone, abnormal intermediate layer, hypertrophic zone, and primary spongiosa, respectively. Boxed regions in H&E and COL10 panels are shown at higher magnification to the right. Scale bars: 50 μm.

hypertrophic differentiation of growth plate chondrocytes (9). To investigate the mechanism underlying cGKII kinase activity in chondrocyte hypertrophy, in the present study we performed a screen of its potential phosphorylation targets and identified glycogen synthase kinase-3β (GSK-3β; encoded by *Gsk3b*) as a significant phosphorylation target of cGKII. Because the phosphorylation of GSK-3β at Ser9 is known to cause its inactivation (10), we further examined the functional involvement of GSK-3β in the cGKII-induced hypertrophic differentiation of chondrocytes and investigated the underlying mechanism. Our results demonstrated that cGKII promotes chondrocyte hypertrophy and skeletal growth through phosphorylation and inactivation of GSK-3β.

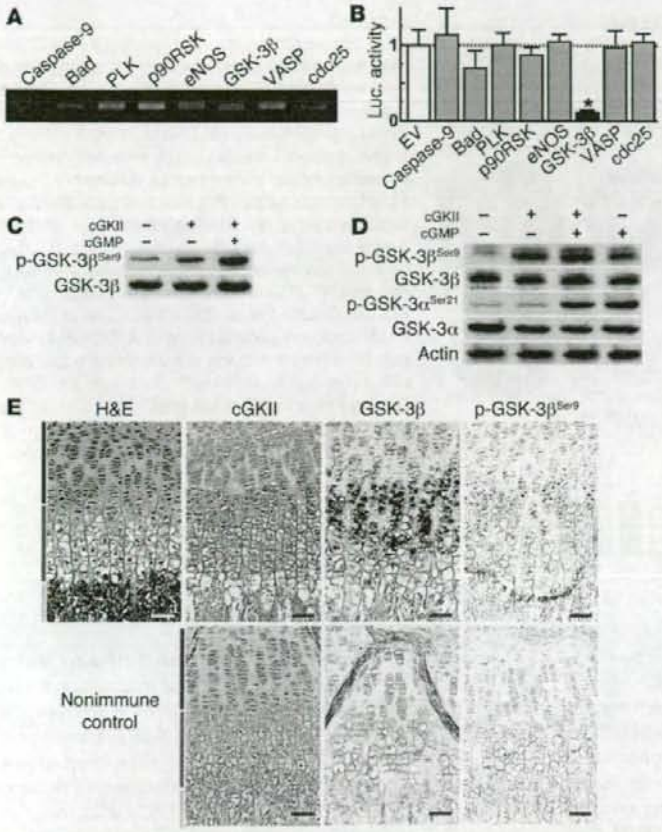

Figure 2

Identification of GSK-3β as a principal phosphorylation target of cGKII during chondrocyte hypertrophy. (**A**) RT-PCR of 8 candidate genes that were identified by the serine/threonine kinase substrate array (Supplemental Table 1) in cultured ATDC5 cells in the prehypertrophic or hypertrophic differentiation stage. (**B**) COL10 promoter activity, as assessed by transfection of the 8 candidate genes or the empty vector (EV) in HuH-7 cells with the luciferase reporter gene construct containing a cloned 4.5-kb promoter fragment of COL10. Data are mean ± SD fold change relative to empty vector. $^*P < 0.01$ versus control. (**C**) In vitro kinase assay of the phosphorylation of recombinant GSK-3β at Ser9 by recombinant cGKII with or without cGMP. Proteins were incubated in the presence of ATP, and the reaction products were analyzed by IB using the same antibody to Ser9-phosphorylated GSK-3β (p-GSK-3β^{Ser9}) as that used in Supplemental Table 1. (**D**) Phosphorylation of endogenous GSK-3β at Ser9 and GSK-3α at Ser21 by cGKII with or without cGMP in ATDC5 cells. Whole-cell lysates were incubated with recombinant cGKII or cGMP in the presence of ATP, and the reaction products were analyzed as in **C**. (**E**) Localization of cGKII, total GSK-3β, and Ser9-phosphorylated GSK-3β, as assessed by immunohistochemistry in the growth plate of proximal tibia in a 2-week-old mouse. Specific stainings were confirmed by immunohistochemistry by respective nonimmune serums (nonimmune control). Blue, green, and yellow bars indicate proliferative zone, hypertrophic zone, and primary spongiosa, respectively. Scale bars: 50 μm.

Results

Growth plate abnormality in Prkg2$^{-/-}$ mice. *Prkg2$^{-/-}$* mice showed postnatal dwarfism with short limbs and trunk compared with WT littermates (Figure 1A), as previously reported (6). Radiographic analysis at 8 weeks of age revealed that the lengths of femur, tibia, and vertebra, which are known to be primarily formed through endochondral ossification, were shorter in *Prkg2$^{-/-}$* mice. The longitudinal length of the *Prkg2$^{-/-}$* skull was also shorter, while the width was comparable to WT. This finding is probably attributable to 2 types of the skull growth via endochondral ossification and intramembranous ossification (11), although this needs to be further investigated. The time course of histological observation of the tibial growth plate revealed that the height was greater in *Prkg2$^{-/-}$* than WT mice from 2 to 4 weeks after birth but was restored to a level comparable to that of WT mice by 8 weeks of age (Figure 1B). As previously observed in KMI rats (9), growth plate elongation during these ages was caused by an abnormal intermediate layer between the proliferative and hypertrophic zones, with accumulation of few proliferative or hypertrophic chondrocytes, as determined by BrdU uptake and expression of type X collagen (COL10), respectively (Figure 1C). The growth plate of the *Prkg2$^{-/-}$* vertebral bones also contained the abnormal intermediate layer, which was intermittently focal in the elongated growth plate (Figure 1D). These results indicate that cGKII is necessary for hypertrophic differentiation of growth plate chondrocytes during endochondral ossification for longitudinal growth of limbs and trunk not only in rats, but also in mice.

Phosphorylation targets of cGKII in chondrocyte hypertrophy. To investigate the mechanism underlying cGKII activity in hypertrophic differentiation of chondrocytes, we performed a screen of its phosphorylation targets by in vitro kinase assay using a serine/threonine kinase substrate array. From 87 candidate peptides containing serine/threonine phosphorylation sites, we identified 8 substrates that were most strongly phosphorylated by cGKII: caspase-9, BCL2-antagonist of cell death (Bad), polo-like kinase (PLK), 90-kDa ribosomal protein S6 kinase (p90RSK), eNOS, GSK-3β, vasodilator-stimulated phosphoprotein (VASP), and cell division cycle 25 homolog (cdc25) (Supplemental Table 1; supplemental material available online with this article; doi:10.1172/JCI35243DS1). All of these molecules were confirmed to be expressed in mouse chondrogenic ATDC5 cells in the prehypertrophic or hypertrophic differentiation stage (Figure 2A). However, a luciferase reporter assay revealed that GSK-3β markedly suppressed COL10 promoter activity, while none of the other candidates had a significant effect (Figure 2B). These data suggest that GSK-3β might be functionally involved in chondrocyte hypertrophy, although involvement of the other factors cannot be ruled out. Direct phosphorylation of recombinant GSK-3β at Ser9, the crucial site for inactivation of GSK-3β (10), by recombinant cGKII protein was confirmed by in vitro kinase assay using the same antibody as the screening array above, and the phos-

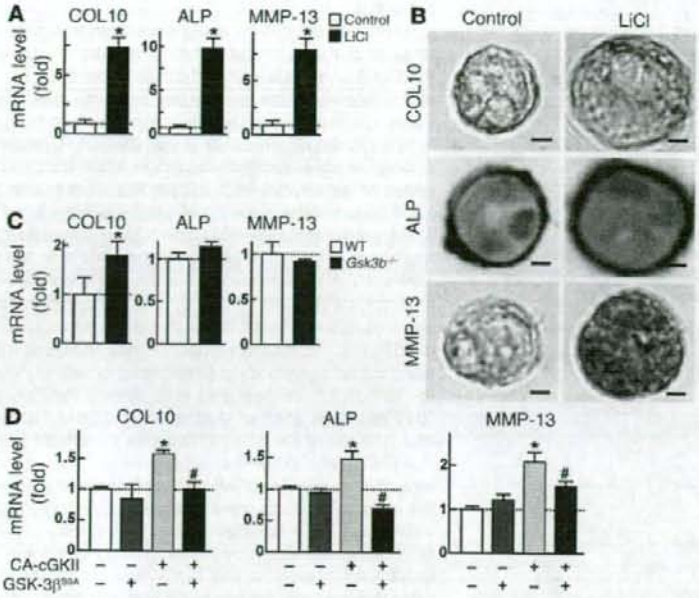

Figure 3
Regulation of chondrocyte hypertrophy by GSK-3β. (**A**) Effects of LiCl on mRNA levels of the hypertrophic markers COL10, ALP, and MMP-13, as assessed by real-time RT-PCR in ATDC5 cells cultured in 3-dimensional alginate beads. (**B**) Effects of LiCl on the hypertrophic markers, as assessed by immunocytochemistry in primary costal chondrocytes cultured in 3-dimensional alginate beads. For morphological comparison, sections of the representative colonies containing 4 cells were selected. Scale bars: 10 μm. (**C**) mRNA levels of the hypertrophic markers, as assessed by real-time RT-PCR in cultured costal chondrocytes from WT and *Gsk3b*$^{+/-}$ mice. (**D**) mRNA levels of the hypertrophic markers in stable lines of ATDC5 cells retrovirally transfected with the constitutively active form of cGKII (CA-cGKII), GSK-3β^{S9A}, or the control GFP (–). Data are mean ± SD of the relative amount compared with control or WT. *$P < 0.01$ versus control or WT. #$P < 0.01$ versus constitutively active cGKII alone.

phorylation was enhanced by the addition of cGMP (Figure 2C). Furthermore, endogenous GSK-3β in cell lysates of ATDC5 cells was phosphorylated at Ser9 by recombinant cGKII protein, which was further enhanced by the addition of cGMP. On the other hand, GSK-3α, the closely related isoform of GSK-3β, was not phosphorylated by cGKII, nor were protein levels of GSK-3β and GSK-3α altered by cGKII or cGMP (Figure 2D). Immunohistochemistry revealed that cGKII, total GSK-3β, and Ser9-phosphorylated GSK-3β were colocalized in prehypertrophic chondrocytes of the growth plate, implicating the interaction of these molecules in vivo as well (Figure 2E). Compared with the respective nonimmune controls, the localization of Ser9-phosphorylated GSK-3β appeared to be restricted to those cells that also produced cGKII, whereas total GSK-3β was more broadly distributed, which supports the notion that cGKII is an important regulator of GSK-3β phosphorylation.

Regulation of chondrocyte hypertrophy by GSK-3β. In the 3-dimensional cultures of ATDC5 cells and primary costal chondrocytes in alginate beads, LiCl, a selective inhibitor of GSK-3β, stimulated the expression of chondrocyte hypertrophic differentiation markers COL10, alkaline phosphatase (ALP), and MMP-13 and induced morphological hypertrophy of the cells (Figure 3, A and B). COL10 expression also increased in cultured primary costal chondrocytes from *Gsk3b*$^{+/-}$ mice compared with WT chondrocytes, while ALP and MMP-13 levels were comparable between the genotypes (Figure 3C). Introduction of a constitutively active allele of cGKII into ATDC5 cells stimulated expression of hypertrophic markers, and this was attenuated by the cointroduction of a phosphorylation-deficient mutant of GSK-3β with a serine-to-alanine substitution (GSK-3β^{S9A}), which is known to have constitutive activity (Figure 3D). These data demonstrated that Ser9 phosphorylation of GSK-3β is necessary for the induction of chondrocyte hypertrophy by cGKII. The GSK-3β^{S9A} introduction alone altered none of the 3 markers (Figure 3D), which indicates that an endogenous GSK-3β level was sufficient for the suppression of chondrocyte hypertrophy in this culture system.

Mechanism underlying cGKII/GSK-3β signaling in chondrocyte hypertrophy. We further examined the molecular mechanism whereby GSK-3β phosphorylation by cGKII regulates hypertrophic differentiation of chondrocytes. Because GSK-3β is known to be a negative regulator of β-catenin through its phosphorylation and degradation (10), we compared the localization of β-catenin, Ser9-phosphorylated GSK-3β, and total GSK-3β in the growth plates of WT and *Prkg2*$^{-/-}$ littermates. In the WT growth plate, β-catenin as well as both GSK-3β proteins were localized mainly in the cytoplasm of prehypertrophic chondrocytes (Figure 4A). cGKII deficiency caused similar decreases in β-catenin and Ser9-phosphorylated GSK-3β levels with little effect on the total GSK-3β level in the abnormal intermediate layer. In cultured ATDC5 cells, cGKII induced cytosolic accumulation of β-catenin after stimulation by 8-bromo-cGMP, while cGKII-Δkinase had a minimal effect (Figure 4B). Overexpression of constitutively active cGKII enhanced the promoter activity of the β-catenin target T cell factor (TCF), which was markedly suppressed by cotransfection of GSK-3β^{S9A} (Figure 4C). Again, GSK-3β^{S9A} alone did not have an effect, which indicates that an endogenous GSK-3β level is sufficient for β-catenin suppression. We next examined the involvement of a scaffolding peptide, Axin, which is known to associate with GSK-3β and promotes effective phosphorylation and degradation of β-catenin under conditions of Wnt stimulation (10). IP/IB analysis using HEK293 cells transfected with Myc-tagged Axin and cGKII revealed that cGKII formed a complex with Axin and phosphorylated GSK-3β not only in the whole-cell lysates, but also in the IP with Axin, suggesting some interaction between Ser9 phosphorylation and coupling with Axin in regulation of GSK-3β by cGKII (Figure 4D).

In our previous study, we showed that cGKII caused attenuation of Sox9 transcriptional function through inhibition of nuclear entry (9). Because Sox9 is known not only to induce chondrogenic differentiation of mesenchymal cells, but also to prevent hypertrophic differentiation of chondrocytes (12), this may contribute

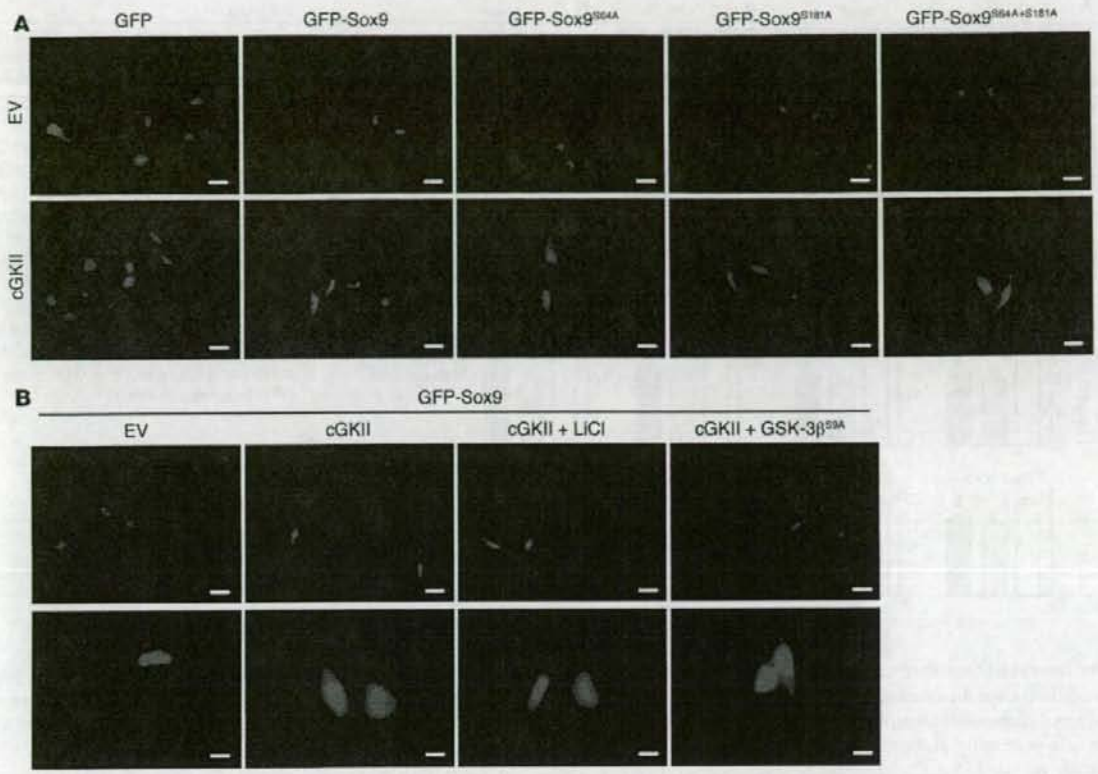

Figure 5
Subcellular localization of Sox9. (**A**) Effect of cGKII on subcellular localization of Sox9 and the phosphorylation-deficient mutants at putative phosphorylation sites at Ser64 ($Sox9^{S64A}$), Ser181 ($Sox9^{S181A}$), or both ($Sox9^{S64A+S181A}$). HeLa cells were transfected with GFP, GFP-tagged Sox9 (GFP-Sox9), or the GFP-tagged mutants in combination with cGKII or empty vector. Subcellular localization of Sox9 or the mutants was determined by a fluorescent microscope. (**B**) Effect of LiCl treatment or $GSK\text{-}3\beta^{S9A}$ transfection on Sox9 subcellular localization in HeLa cells cotransfected with GFP-tagged Sox9 in combination with cGKII or empty vector. Scale bars: 10 μm (**A**); 20 μm (**B**, top); 5 μm (**B**, bottom).

membranous ossification (11, 18) – were comparable to those of WT littermates (Figure 6C). The genetic insufficiency of GSK-3β in the $Prkg2^{-/-}Gsk3b^{+/-}$ mice partially, but significantly, restored the impaired skeletal growth (about 20%–40%). These findings indicate that sufficient GSK-3β function is needed for skeletal growth and endochondral ossification to be impaired by cGKII deficiency.

Further histological analyses revealed that the elongated growth plate and decreased COL10 expression in $Prkg2^{-/-}$ mice were also partially restored in the $Prkg2^{-/-}Gsk3b^{+/-}$ mice (Figure 7, A and B). In contrast, GSK-3β insufficiency did not alter skeletal growth or growth plate parameters in WT or $Prkg2^{+/-}$ mice, as shown in $Gsk3b^{+/-}$ and compound $Prkg2^{+/-}Gsk3b^{+/-}$ mice, respectively (Supplemental Figure 3). GSK-3β may therefore function specifically as a mediator of cGKII signaling, rather than generally in the regulation of chondrocyte hypertrophy and endochondral ossification.

Discussion

Based on our previous finding that cGKII activity is essential for the promotion of skeletal growth through hypertrophic differentiation of growth plate chondrocytes (9), the results of our present study initially identified GSK-3β as a likely substrate of this protein kinase. Figure 7C summarizes the mechanism underlying chondrocyte hypertrophy by cGKII/GSK-3β signaling based on the present and previous studies. cGKII phosphorylates GSK-3β at Ser9 and inactivates it, which may contribute to the suppression of β-catenin degradation, as previously reported (10). We and others have reported that β-catenin/TCF signaling causes stimulation of hypertrophic differentiation of chondrocytes in vitro (19–22). In addition, chondrocyte-specific inactivation of β-catenin in mice results in dwarfism with delayed hypertrophic differentiation of chondrocytes (23). Hence, the stabilization and accumulation of β-catenin by cGKII/GSK-3β signaling in chondrocytes may lead to hypertrophic differentiation, although the underlying molecular mechanism is still controversial.

Genetic rescue of impaired skeletal growth in $Prkg2^{-/-}$ mice by suppression of GSK-3β was significant, but incomplete (Figures 6 and 7). This might be because GSK-3β haploinsufficiency was inadequate to fully overcome the deficiency of cGKII. Indeed, cultured $Gsk3b^{+/-}$ chondrocytes showed higher COL10 expression, but similar ALP and MMP-13 expression, compared with WT cells, while LiCl clearly increased all hypertrophic markers in the ATDC5 cell culture (Figure 3, A and C). We cannot exclude the possibil-

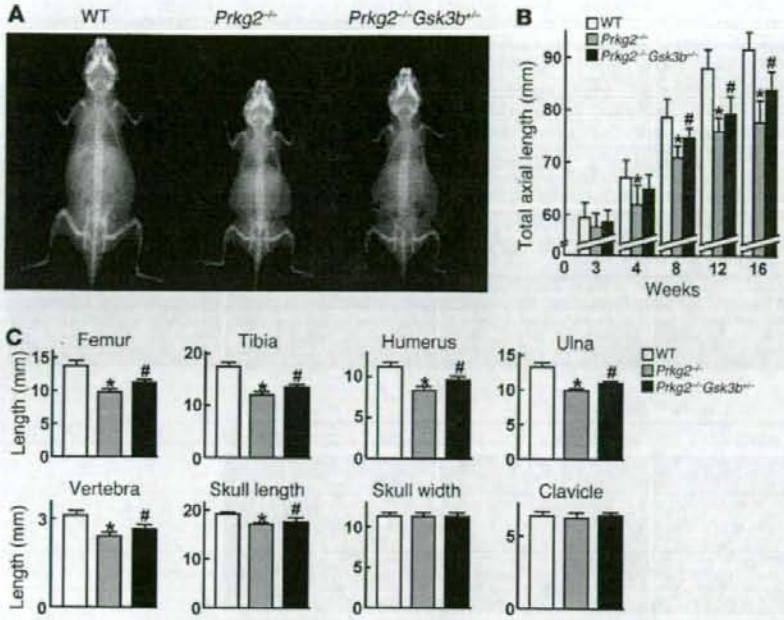

Figure 6
Genetic rescue of growth retardation in *Prkg2*$^{-/-}$ mice by GSK-3β insufficiency. (**A**) Radiographs of WT, *Prkg2*$^{-/-}$, and *Prkg2*$^{-/-}$ *Gsk3b*$^{+/-}$ littermates at 8 weeks of age. (**B**) Time course of total axial length (from nose to tail end) of the 3 genotypes from 3 to 16 weeks of age. The recovery by the GSK-3β insufficiency in the *Prkg2*$^{-/-}$ mice was 43.2%, 31.4%, and 41.9% at 8, 12, and 16 weeks, respectively. (**C**) Length of bones of the 3 genotypes at 8 weeks of age. Percent recovery was 21.7%, 18.3%, 24.3%, 16.2%, 24.3%, and 42.6% in femur, tibia, humerus, ulna, vertebra, and skull length, respectively. Data are mean ± SD for 4–9 mice per genotype. $^{*}P < 0.05$ versus WT. $^{\#}P < 0.05$ versus *Prkg2*$^{-/-}$.

ity, however, of involvement of other mechanisms in the actions of cGKII on chondrocyte hypertrophy. Although our previous study showed that cGKII phosphorylated Sox9, an inhibitor of chondrocyte hypertrophy, and suppressed its nuclear entry (9), the present study revealed that the subcellular translocation was not mediated by the phosphorylation of Sox9 itself or of GSK-3β (Figure 5). Besides Sox9 and GSK-3β, VASP and cysteine- and glycine-rich protein 2 have previously been reported as phosphorylation targets of cGKII in other types of cells (24). However, our luciferase assays failed to show regulation of COL10 transcription by either gene (Figure 2B and Supplemental Figure 2B), suggesting the existence of other phosphorylation targets of cGKII in the regulation of Sox9 translocation associated with chondrocyte hypertrophy. In addition, because Sox9 has previously been reported to physically interact with β-catenin and to compete with its binding to TCF (23), the downstream pathways of cGKII through GSK-3β and Sox9 might interact at the level of β-catenin during chondrocyte hypertrophy.

Chondrocyte hypertrophy in the growth plate is a rate-limiting step for longitudinal skeletal growth (25), because this step has been shown to be responsible for 40%–60% of endochondral ossification, with the remainder caused by chondrocyte proliferation and matrix synthesis (26). Sox9 is a representative regulator of this step, as are Runx2 (1, 13) and parathyroid hormone/parathyroid hormone–related protein (PTH/PTHrP) (1, 27), uncovered via recent advances in molecular genetics. The present study failed to find interaction between cGKII and Runx2 (Supplemental Figure 1). Although PTH/PTHrP has previously been shown to be a potent inhibitor of chondrocyte hypertrophy by the findings in deficient and transgenic mice (1, 27), our previous study revealed that neither expression levels of PTHrP and PTH/PTHrP receptor nor cAMP accumulation by PTH stimulation was altered by cGKII deficiency in chondrocytes (9). Hence, cGKII may regulate chondrocyte hypertrophy by a mechanism independent of those of Runx2 and PTH/PTHrP.

In line with the view that cGKII is a downstream mediator of CNP, *Nppc*$^{-/-}$ and *Npr2*$^{-/-}$ mice also exhibit dwarfism (2). However, unlike *Prkg2*$^{-/-}$ mice, which have an elongated growth plate with an abnormal intermediate layer, both *Nppc*$^{-/-}$ mice and *Npr2*$^{-/-}$ mice showed thinned growth plates with chondrocytes arranged in a regular columnar array. This may indicate the involvement of other signaling pathways in CNP/GC-B–mediated endochondral ossification. In fact, the intracellular accumulation of cGMP caused by CNP/GC-B signaling activates not only cGKII, but also other downstream mediators, such as cGKI, cyclic nucleotide phosphodiesterases, and cGMP-regulated ion channels (5, 28). Although no skeletal abnormality has been reported in *Prkg1*$^{-/-}$ mice (8), it would be helpful to investigate whether mice doubly deficient for cGKI and cGKII mimic the phenotype of *Nppc*$^{-/-}$ or *Npr2*$^{-/-}$ mice. In addition, targeted overexpression of CNP in growth plate chondrocytes was reported to restore the achondroplastic bone with FGF receptor 3 mutation through inhibition of the MAPK pathway (15), which we found in the present study to be unrelated to cGKII (Supplemental Figure 2A). Furthermore, cGKII functions as an effector of cGMP that is activated not only by CNP, but also by nitric oxide and other types of natriuretic peptides (5, 7, 28). Although the fact that CNP was unable to affect chondrocyte differentiation of skeletal growth in the absence of cGKII either in vitro or in vivo indicates a crucial role of cGKII in CNP signaling (29), CNP and cGKII are unlikely to function with a one-to-one correspondence during endochondral ossification.

The abnormal elongation of the *Prkg2*$^{-/-}$ mouse growth plate was apparent from 2 to 4 weeks after birth, but not before or after these ages (Figure 1B). This observation suggests some compensatory mechanisms for cGKII deficiency. Besides signaling via Runx2, PTH/PTHrP, and the CNP-related factors described above, GSK-3α (the other GSK-3 in mammals) might substitute for GSK-3β, because it was not found to be a phosphorylation target of cGKII (Figure 2D). Although there was no compensatory upregulation in

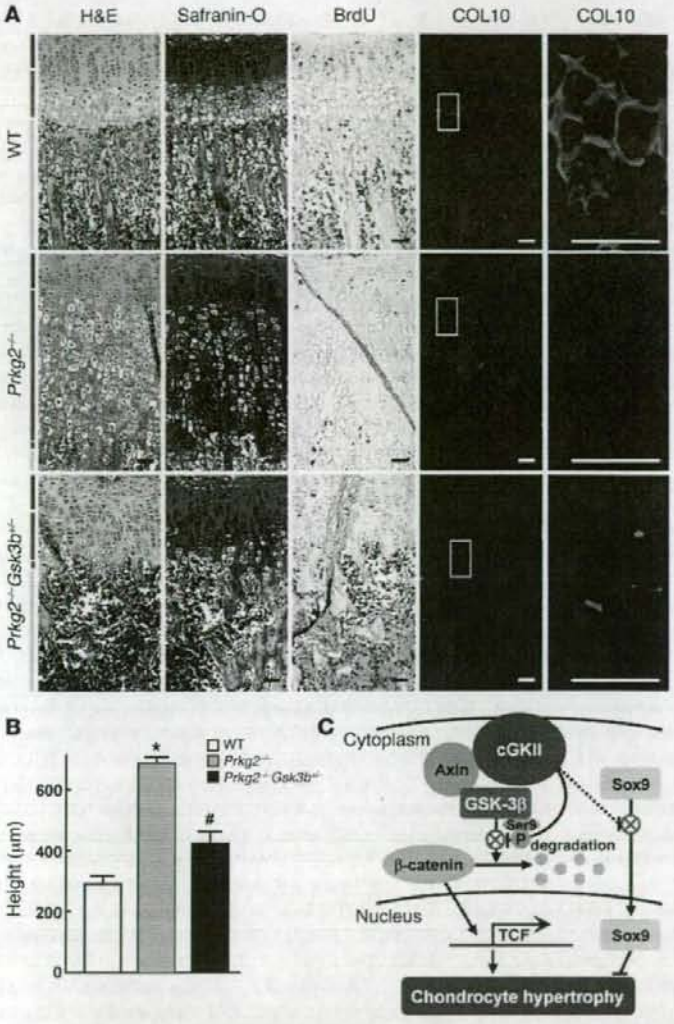

Figure 7
Genetic rescue of growth plate abnormality in *Prkg2*$^{-/-}$ mice by GSK-3β insufficiency. (**A**) H&E staining, Safranin-O staining, BrdU labeling, and immunohistochemical staining of COL10 in the tibial growth plates of 3-week-old mice of the 3 genotypes. Blue, red, green, and yellow bars indicate proliferative zone, abnormal intermediate layer, hypertrophic zone, and primary spongiosa, respectively. Boxed regions in COL10 panels are shown at higher magnification to the right. Scale bars: 50 μm. (**B**) Height of the growth plates of the 3 genotypes. The percentage recovery by the GSK-3β insufficiency was 36.0%. Data are mean ± SD of 4 mice per genotype. $^{*}P < 0.05$ versus WT, $^{\#}P < 0.05$ versus *Prkg2*$^{-/-}$. (**C**) Schematic of the mechanism whereby cGKII promotes growth plate chondrocyte hypertrophy during skeletal growth.

GSK-3 levels in cells lacking either GSK-3α or GSK-3β, functional redundancy of the 2 GSK-3 homologs in β-catenin/TCF–mediated transcription was previously shown using an allelic series of embryonic stem cell lines (17, 30). In fact, *Gsk3b*$^{+/-}$ mice (Supplemental Figure 3) and *Gsk3a*$^{-/-}$ mice (31) showed normal skeletal development and growth. *Gsk3b*$^{-/-}$ mice developed relatively normally until late gestation, when massive liver apoptosis causes embryonic lethality (17); the implication of this finding is that GSK-3α can compensate for GSK-3β deficiency in early stages of mouse development, but cannot substitute for it in all respects. Hence, the age-dependent balance between GSK-3α and GSK-3β might explain the temporary growth plate abnormality in *Prkg2*$^{-/-}$ mice.

GSK-3β is known to be active under resting conditions and inactivated upon stimulation by several signaling pathways, such as Wnt and insulin/Akt; however, the role of phosphorylation of GSK-3β remains controversial (32, 33). Our present results led us to propose cGKII as a novel regulator of GSK-3β and showed that the β-catenin activity enhanced by cGKII was suppressed by GSK-3β^{S9A}, indicating the mediation of GSK-3β phosphorylation at Ser9 in cGKII/β-catenin signaling (Figure 4C). Conversely, several reports showed that GSK-3β inactivation causing β-catenin induction by Wnt stimulation depends not on Ser9 phosphorylation, but rather on coupling with the scaffolding protein, such as Axin (34, 35). The present study, however, showed that cGKII formed a complex with Axin and further phosphorylated GSK-3β that bound to Axin (Figure 4D), suggesting some interaction between Ser9 phosphorylation and coupling with Axin in the regulation of GSK-3β by cGKII. In fact, a previous report proposed that Wnt signaling, similar to insulin/Akt signaling, induces GSK-3β phosphorylation via the interaction between the signaling pathways both in neuronal PC12 cells and in human embryonic kidney 293T cells (36). While these findings imply a possible link between cGKII/β-catenin and canonical Wnt/β-catenin signaling, we note that there is no direct evidence of cGKII being involved in the canonical Wnt pathway. We therefore believe that cGKII/β-catenin signaling, which is dependent on GSK-3β phosphorylation, may have a mechanism that is, at least in part, distinct from that of Wnt/β-catenin signaling. Further studies will be needed to clarify the details of GSK-3β–related signaling not only in chondrocytes, but also in other cells.

We conclude that cGKII promotes chondrocyte hypertrophy and skeletal growth through phosphorylation and inactivation of GSK-3β. For the application of this intracellular signaling to yield novel therapeutics for skeletal disorders, we are now developing a gene transfer system using biocompatible polyplex nanomicelles (37, 38). Further understanding of the molecular signaling related to the cGKII/GSK-3β axis, in combination with other putative signaling systems, will greatly assist in unraveling the molecular network that modulates endochondral ossification and skeletal growth.

Methods

Animals. The *Prkg2*$^{-/-}$ mice and *Gsk3b*$^{+/-}$ mice were maintained in a C57BL/6 background. To generate *Prkg2*$^{-/-}$ *Gsk3b*$^{+/-}$ mice, *Gsk3b*$^{+/-}$ mice were mated with the homozygous *Prkg2*$^{-/-}$ mice to obtain *Prkg2*$^{+/-}$ *Gsk3b*$^{+/-}$ mice, which were then mated with each other. All experiments were performed on male mice and were approved by the Animal Care and Use Committee of the University of Tokyo.

Radiological and histological analyses. Plain radiographs were taken using a soft X-ray apparatus (Softex CMB-2; Softex). For histological analyses, skeletons were fixed in 4% paraformaldehyde, decalcified with 10% EDTA, embedded in paraffin, sectioned in 5-μm slices, and stained with H&E or Safranin-O, according to standard procedures. For BrdU labeling, mice were injected intraperitoneally with BrdU (25 μg/g body weight) 2 h prior to sacrifice, and the sections were stained with a BrdU staining kit (Zymed Laboratories) according to the manufacturer's instructions. In situ hybridization with nonradioactive probes was performed as previously described (39). For immunohistochemistry, antibodies to cGKII, Ser9-phosphorylated GSK-3β, MMP-13, Runx2 (1:50; Santa Cruz Biotechnology Inc.), GSK-3β (1:200; Chemicon), COL10 (1:1000; LSL), β-catenin (1:100; Cell Signaling Technology), and respective nonimmune serums were used, and the signal was detected with an HRP-conjugated secondary antibody. For fluorescent visualization, a secondary antibody conjugated with Alexa Fluor 488 (Invitrogen) was used.

Cell cultures. ATDC5 cells were grown and maintained in DMEM and F12 at a 1:1 ratio with 5% FBS. To induce hypertrophic differentiation, the ATDC5 cells were cultured in the presence of insulin, transferrin and sodium selenite (ITS) supplement (Sigma-Aldrich) for 21 d as described previously (40). We confirmed COL10 expression by real-time RT-PCR and used the cells whose stage of differentiation was assumed to be prehypertrophic or hypertrophic. Primary chondrocytes were isolated by digestion of E18.5 costal cartilage. Primary chondrocytes, HuH-7 cells, HEK293 cells, and HeLa cells were cultured in high-glucose DMEM with 10% FBS. Three-dimensional alginate bead cultures of primary costal chondrocytes and ATDC5 cells were performed with or without LiCl (8 mM) for 72 h, and the cells were analyzed as described previously (21). For immunocytochemistry of primary costal chondrocytes, the cell colonies were fixed with 4% paraformaldehyde, embedded in paraffin, sectioned in 5-μm slices, and underwent immunostaining for COL10 and MMP-13 as described above. For ALP staining, sections were fixed in 70% ethanol and stained for 10 min with a solution containing 0.01% Naphthol AS-MX phosphate disodium salt (Sigma-Aldrich), 1% N, N-dimethyl-formamide (Wako Pure Chemical Industries Ltd.), and 0.06% fast blue BB (Sigma-Aldrich).

In vitro kinase assay. ATDC5 cells were cultured in the presence of ITS for 21 d to differentiate into prehypertrophic or hypertrophic chondrocytes, as described above. The whole-cell lysate of the differentiated cells was prepared using Cell Lysis Buffer (Cell Signaling Technology). The cell lysate or recombinant GSK-3β (Upstate Biotechnology Inc.) was incubated with recombinant cGKII (Sigma-Aldrich) in a reaction buffer (Cell Signaling Technology) containing 1.6 mM ATP and 100 μM 8-bromo-cGMP (Biomol) at 30°C for 30 min. An equal amount of protein (15 μg) was subjected to SDS-PAGE and transferred onto nitrocellulose membranes. IB was then performed using primary antibodies to Ser9-phosphorylated GSK-3β (Cell Signaling Technology), GSK-3β (Chemicon), Ser21-phosphorylated GSK-3α and GSK-3α (Cell Signaling Technology), and β-actin (Sigma-Aldrich). The membrane was incubated with HRP-conjugated antibody (Promega), and the immunoreactive proteins were visualized with ECL Plus (Amersham Biosciences).

Plasmids and viral vectors. cDNA of caspase-9 (GenBank accession no. NM_001229.1), Bad (NM_007522.2), PLK (NM_011121.3), p90RSK (NM_009097.4), eNOS (NM_000603.3), GSK-3β (NM_002093.2), VASP (NM_009499.1), cdc25 (NM_009860.2), and cysteine- and glycine-rich protein 2 (CSRP2; NM_007792.3) was ligated into pCMV-HA (Invitrogen). cDNA of rat cGKII (NM_013012.1; nucleotides 48–2,333) was ligated into pcDNA4HisA (Invitrogen). A PCR-amplified fragment (nucleotides 48–1,403) was used to construct the cGKII-Δkinase plasmid. Plasmids encoding constitutively active human cGKII were kindly provided by B.M. Hogema (Erasmus University Medical Center, Rotterdam, The Netherlands; ref. 41). Axin1 (NM_003502.2) was subcloned into pCMV-Myc (Invitrogen) to introduce Myc epitope tags. cDNA of Sox9 (NM_000346.2) and Runx2 (NM_009820.3) was ligated into pEGFPC1 (Clontech) to generate GFP-tagged plasmids. To create phosphorylation-deficient mutants, GFP-tagged Sox9 plasmid and GSK-3β plasmid were subjected to site-directed mutagenesis using the inverse PCR technique. All constructs were verified by sequencing. cGKII, cGKII-Δkinase, GSK-3β^{S9A}, and control GFP retrovirus vectors were constructed using pMx vector and plat-E cells as described previously (42).

Gene transfection. For the transient transfection, a total of 1 μg plasmid DNA was transfected using Fugene6 (Roche). For cotransfection, all plasmids were added in an equal ratio. Total RNA was isolated 72 h after the transfection and used for the subsequent assays. For fluorescent detection, HeLa cells were transiently transfected, and fluorescent images were taken 24 h after transfection. To investigate the interaction of cGKII and MAPK/STAT signaling, ATDC5 cells were transfected with cGKII or the empty vector, and FGF-2 (1 ng/ml) was added 72 h after transfection. IB was then carried out using primary antibodies to p-Erk1/2, Erk1/2, p-p38MAPK, p38MAPK, p-JNK2/3, JNK2/3, p-JNK1, JNK1, p-STAT1, and STAT1 (Cell Signaling Technology) as described above.

Real-time RT-PCR. Total RNA was reverse-transcribed with MultiScribe RT (Applied Biosystems Inc.). Semiquantitative RT-PCR was performed within an exponential phase of the amplification, with the following primer sequences: caspase-9 forward, 5′-CGATGCAGGGTGCGCCTAGTGA-3′; caspase-9 reverse, 5′-TGACCAGCTGCCTGGCCTGATC-3′; Bad forward, 5′-CCAGGTCTCCTGGGGAGCAACATTC-3′; Bad reverse, 5′-AGCTCCTCCTCCATCCCTTCATCC-3′; PLK forward, 5′-TGGCACTCCTAACTACATAGCTCCTGAGG-3′; PLK reverse, 5′-CGGAGGTAGGTCTCTTTTAGGCACGA-3′; p90RSK forward, 5′-GATTCTTCTGCGGTATGGCCA-3′; p90RSK reverse, 5′-TGCCGTAGGATCTTATCCAGCA-3′; eNOS forward, 5′-CTCGAGTGGTTTGCTGCCCTTG-3′; eNOS reverse, 5′-CAGGTCCCTCATGCCAATCTCTGA-3′; GSK-3β forward, 5′-CCAGTATAGATGTATGGTCTG-3′; GSK-3β reverse, 5′-CTTGTTGGTGTTCCTAGG-3′; VASP forward, 5′-TTCCAGCCGGGCTACTGTGATG-3′; VASP reverse, 5′-CGGCCAACAACTCGGAAGGAGT-3′; cdc25 forward, 5′-GCACTGGAAAGGGTGGAGAGACTGG-3′; cdc25 reverse, 5′-CCTCTTCACTTGCAGGTGGGATAGG-3′; Runx2 forward, 5′-CCCAGCCACCTTTACCTACA-3′; Runx2 reverse, 5′-TATGGAGTGCTGCTGGTCTG-3′. Real-time RT-PCR was performed on an ABI 7700 Sequence Detection system (Applied Biosystems) using QuantiTect SYBR Green PCR Master Mix (Qiagen) with β-actin as the internal control and the following primer sequences: COL10 forward, 5′-CATAAAGGGCCCACTTGCTA-3′; COL10 reverse, 5′-TGGCTGATATTCCTGGTGGT-3′; ALP forward, 5′-GCTGATCATTCCCACGTTTT-3′; ALP reverse, 5′-CTGGGCCTGGTAGTTGTTGT-3′; MMP-13 forward, 5′-AGGCCTTCAGAAAAGCCTTC-3′; MMP-13 reverse, 5′-TCCTTGGAGTGATCCAGACC-3′; β-actin forward, 5′-AGATGTGGATCAGCAAGCAG-3′; β-actin reverse, 5′-GCGCAAGTTAGGTTTTGTCA-3′. All reactions were run in triplicate.

Luciferase reporter gene assay. The human COL10 promoter regions from −4,459 bp relative to the transcriptional start site were cloned into the pGL3-Basic vector (Promega). The TOPflash system (Upstate Biotechnology Inc.) was used according to the manufacturer's protocol. The luciferase assay was performed with a dual-luciferase reporter assay system (Promega) using a GloMax 96 Microplate Luminometer (Promega).

IP and IB assay. IP was performed with ProFound Myc Tag IP/Co-IP kits (Pierce) according to the manufacturer's protocol. Samples were prepared using M-PER or NE-PER (Pierce) supplemented with 2 mM Na_3VO_4 and 10 mM NaF according to the manufacturer's protocol. Cell lysates were incubated with the high-affinity anti-c-Myc antibody–coupled agarose

at 4°C overnight. Immunocomplexes were washed 3 times with cold wash solution. c-Myc-tagged proteins were eluted, and an equal amount of each eluted sample (15 μg) was subjected to SDS-PAGE, transferred onto nitrocellulose membranes, and subjected to IB using primary antibodies to cGKII (Santa Cruz Biotechnology Inc.), GSK-3β and Ser9-phosphorylated GSK-3β (Chemicon), and Myc tag (Upstate Biotechnology Inc.). Immunoreactive proteins were visualized as described above.

Statistics. Means of groups were compared by ANOVA, and significance of differences was determined by post-hoc testing by the Bonferroni method. A P value less than 0.05 was considered significant.

Acknowledgments

We thank Boris M. Hogema for providing plasmids encoding constitutively active human cGKII; Henry Kronenberg and Sakae Tanaka for critical discussions; and Reiko Yamaguchi and Mizue Ikeuchi for their excellent technical help. This work was supported by Grant-in-Aid no. 14657359 for Scientific Research from the Japanese Ministry of Education, Culture, Sports, Science and Technology.

Received for publication February 5, 2008, and accepted in revised form May 7, 2008.

Address correspondence to: Hiroshi Kawaguchi, Sensory and Motor System Medicine, Faculty of Medicine, University of Tokyo, Hongo 7-3-1, Bunkyo-ku, Tokyo 113-8655, Japan. Phone: 81-33815-5411 ext. 30473; Fax: 81-33818-4082; E-mail: kawaguchi-ort@h.u-tokyo.ac.jp.

1. Kronenberg, H.M. 2003. Developmental regulation of the growth plate. *Nature.* **423**:332–336.
2. Chusho, H., et al. 2001. Dwarfism and early death in mice lacking C-type natriuretic peptide. *Proc. Natl. Acad. Sci. U. S. A.* **98**:4016–4021.
3. Tamura, N., et al. 2004. Critical roles of the guanylyl cyclase B receptor in endochondral ossification and development of female reproductive organs. *Proc. Natl. Acad. Sci. U. S. A.* **101**:17300–17305.
4. Bartels, C.F., et al. 2004. Mutations in the transmembrane natriuretic peptide receptor NPR-B impair skeletal growth and cause acromesomelic dysplasia, type Maroteaux. *Am. J. Hum. Genet.* **75**:27–34.
5. Schulz, S. 2005. C-type natriuretic peptide and guanylyl cyclase B receptor. *Peptides.* **26**:1024–1034.
6. Pfeifer, A., et al. 1996. Intestinal secretory defects and dwarfism in mice lacking cGMP-dependent protein kinase II. *Science.* **274**:2082–2086.
7. Pfeifer, A., et al. 1999. Structure and function of cGMP-dependent protein kinases. *Rev. Physiol. Biochem. Pharmacol.* **135**:105–149.
8. Pfeifer, A., et al. 1998. Defective smooth muscle regulation in cGMP kinase I-deficient mice. *EMBO J.* **17**:3045–3051.
9. Chikuda, H., et al. 2004. Cyclic GMP-dependent protein kinase II is a molecular switch from proliferation to hypertrophic differentiation of chondrocytes. *Genes Dev.* **18**:2418–2429.
10. Doble, B.W., and Woodgett, J.R. 2003. GSK-3: tricks of the trade for a multi-tasking kinase. *J. Cell Sci.* **116**:1175–1186.
11. Holmbeck, K. 2005. Collagenase in cranial morphogenesis. *Cells Tissues Organs.* **181**:154–165.
12. Akiyama, H., Chaboissier, M.C., Martin, J.F., Schedl, A., and de Crombrugghe, B. 2002. The transcription factor Sox9 has essential roles in successive steps of the chondrocyte differentiation pathway and is required for expression of Sox5 and Sox6. *Genes Dev.* **16**:2813–2828.
13. Takeda, S., Bonnamy, J.P., Owen, M.J., Ducy, P., and Karsenty, G. 2001. Continuous expression of Cbfa1 in nonhypertrophic chondrocytes uncovers its ability to induce hypertrophic chondrocyte differentiation and partially rescues Cbfa1-deficient mice. *Genes Dev.* **15**:467–481.
14. Ornitz, D.M. 2005. FGF signaling in the developing endochondral skeleton. *Cytokine Growth Factor Rev.* **16**:205–213.
15. Yasoda, A., et al. 2004. Overexpression of CNP in chondrocytes rescues achondroplasia through a MAPK-dependent pathway. *Nat. Med.* **10**:80–86.
16. Deng, C., Wynshaw-Boris, A., Zhou, F., Kuo, A., and Leder, P. 1996. Fibroblast growth factor receptor 3 is a negative regulator of bone growth. *Cell.* **84**:911–921.
17. Hoeflich, K.P., et al. 2000. Requirement for glycogen synthase kinase-3beta in cell survival and NF-kappaB activation. *Nature.* **406**:86–90.
18. Huang, L.F., Fukai, N., Selby, P.B., Olsen, B.R., and Mundlos, S. 1997. Mouse clavicular development: analysis of wild-type and cleidocranial dysplasia mutant mice. *Dev. Dyn.* **210**:33–40.
19. Dong, Y.F., Soung do, Y., Schwarz, E.M., O'Keefe, R.J., and Drissi, H. 2006. Wnt induction of chondrocyte hypertrophy through the Runx2 transcription factor. *J. Cell Physiol.* **208**:77–86.
20. Hartmann, C., and Tabin, C.J. 2000. Dual roles of Wnt signaling during chondrogenesis in the chicken limb. *Development.* **127**:3141–3159.
21. Yano, F., et al. 2005. The canonical Wnt signaling pathway promotes chondrocyte differentiation in a Sox9-dependent manner. *Biochem. Biophys. Res. Commun.* **333**:1300–1308.
22. Tamamura, Y., et al. 2005. Developmental regulation of Wnt/beta-catenin signals is required for growth plate assembly, cartilage integrity, and endochondral ossification. *J. Biol. Chem.* **280**:19185–19195.
23. Akiyama, H., et al. 2004. Interactions between Sox9 and beta-catenin control chondrocyte differentiation. *Genes Dev.* **18**:1072–1087.
24. Schlossmann, J., and Hofmann, F. 2005. cGMP-dependent protein kinases in drug discovery. *Drug Discov. Today.* **10**:627–634.
25. Hunziker, E.B. 1994. Mechanism of longitudinal bone growth and its regulation by growth plate chondrocytes. *Microsc. Res. Tech.* **28**:505–519.
26. Wilsman, N.J., Farnum, C.E., Leiferman, E.M., Fry, M., and Barreto, C. 1996. Differential growth by growth plates as a function of multiple parameters of chondrocytic kinetics. *J. Orthop. Res.* **14**:927–936.
27. Kronenberg, H.M. 2006. PTHrP and skeletal development. *Ann. N. Y. Acad. Sci.* **1068**:1–13.
28. Pilz, R.B., and Casteel, D.E. 2003. Regulation of gene expression by cyclic GMP. *Circ. Res.* **93**:1034–1046.
29. Miyazawa, T., et al. 2002. Cyclic GMP-dependent protein kinase II plays a critical role in C-type natriuretic peptide-mediated endochondral ossification. *Endocrinology.* **143**:3604–3610.
30. Doble, B.W., Patel, S., Wood, G.A., Kockeritz, L.K., and Woodgett, J.R. 2007. Functional redundancy of GSK-3alpha and GSK-3beta in Wnt/beta-catenin signaling shown by using an allelic series of embryonic stem cell lines. *Dev. Cell.* **12**:957–971.
31. MacAulay, K., et al. 2007. Glycogen synthase kinase 3alpha-specific regulation of murine hepatic glycogen metabolism. *Cell Metab.* **6**:329–337.
32. Patel, S., Doble, B., and Woodgett, J.R. 2004. Glycogen synthase kinase-3 in insulin and Wnt signalling: a double-edged sword? *Biochem. Soc. Trans.* **32**:803–808.
33. Dominguez, I., and Green, J.B. 2001. Missing links in GSK3 regulation. *Dev. Biol.* **235**:303–313.
34. Papadopoulou, D., Bianchi, M.W., and Bourouis, M. 2004. Functional studies of shaggy/glycogen synthase kinase 3 phosphorylation sites in Drosophila melanogaster. *Mol. Cell. Biol.* **24**:4909–4919.
35. Ding, V.W., Chen, R.H., and McCormick, F. 2000. Differential regulation of glycogen synthase kinase 3beta by insulin and Wnt signaling. *J. Biol. Chem.* **275**:32475–32481.
36. Fukumoto, S., et al. 2001. Akt participation in the Wnt signaling pathway through Dishevelled. *J. Biol. Chem.* **276**:17479–17483.
37. Itaka, K., et al. 2007. Bone regeneration by regulated in vivo gene transfer using biocompatible polyplex nanomicelles. *Mol. Ther.* **15**:1655–1662.
38. Ohba, S., et al. 2007. Identification of a potent combination of osteogenic genes for bone regeneration using embryonic stem (ES) cell-based sensor. *FASEB J.* **21**:1777–1787.
39. Kamekura, S., et al. 2006. Contribution of runt-related transcription factor 2 to the pathogenesis of osteoarthritis in mice after induction of knee joint instability. *Arthritis Rheum.* **54**:2462–2470.
40. Shukunami, C., et al. 1997. Cellular hypertrophy and calcification of embryonal carcinoma-derived chondrogenic cell line ATDC5 in vitro. *J. Bone Miner. Res.* **12**:1174–1188.
41. Vaandrager, A.B., et al. 2003. Autophosphorylation of cGMP-dependent protein kinase type II. *J. Biol. Chem.* **278**:28651–28658.
42. Saito, T., Ikeda, T., Nakamura, K., Chung, U.I., and Kawaguchi, H. 2007. S100A1 and S100B, transcriptional targets of SOX trio, inhibit terminal differentiation of chondrocytes. *EMBO Rep.* **8**:504–509.

THE JOURNAL OF BIOLOGICAL CHEMISTRY VOL. 283, NO. 39, pp. 26499–26508, September 26, 2008
Printed in the U.S.A.

Pivotal Role of Bcl-2 Family Proteins in the Regulation of Chondrocyte Apoptosis*[S]

Received for publication, February 5, 2008, and in revised form, July 16, 2008 Published, JBC Papers in Press, July 16, 2008, DOI 10.1074/jbc.M800933200

Yasushi Oshima[‡], Toru Akiyama[‡], Atsuhiko Hikita[§], Mitsuyasu Iwasawa[‡], Yuichi Nagase[‡], Masaki Nakamura[‡], Hidetoshi Wakeyama[‡], Naohiro Kawamura[‡], Toshiyuki Ikeda[‡], Ung-il Chung[¶], Lothar Hennighausen[‖], Hiroshi Kawaguchi[‡], Kozo Nakamura[‡], and Sakae Tanaka[‡1]

From the [‡]Department of Orthopaedic Surgery, Faculty of Medicine, the University of Tokyo, 7-3-1 Hongo, Bunkyo-ku, Tokyo 113-0033, Japan, the [§]Department of Pathomechanisms, Clinical Research Center, National Hospital Organization Sagamihara Hospital, 18-1 Sakuradai, Sagamihara, Kanagawa 228-8522, Japan, [¶]Center for Disease Biology and Integrative Medicine, the University of Tokyo, 7-3-1 Hongo, Bunkyo-ku, Tokyo 113-0033, Japan, and [‖]Laboratory of Genetics and Physiology, National Institutes of Health, Bethesda, Maryland 20892-2560

During endochondral ossification, chondrocytes undergo hypertrophic differentiation and die by apoptosis. The level of inorganic phosphate (P_i) elevates at the site of cartilage mineralization, and when chondrocytes were treated with P_i, they underwent rapid apoptosis. Gene silencing of the proapoptotic Bcl-2 homology 3-only molecule *bnip3* significantly suppressed P_i-induced apoptosis. Conversely, overexpression of Bcl-xL suppressed, and its knockdown promoted, the apoptosis of chondrocytes. Bnip3 was associated with Bcl-xL in chondrocytes stimulated with P_i. Bcl-xL was expressed uniformly in the growth plate chondrocytes, whereas Bnip3 expression was exclusively localized in the hypertrophic chondrocytes. Finally, we generated chondrocyte-specific *bcl-x* knock-out mice using the Cre-loxP recombination system, and we provided evidence that the hypertrophic chondrocyte layer was shortened in those mice because of an increased apoptosis of prehypertrophic and hypertrophic chondrocytes, with the mice afflicted with dwarfism as a result. These results suggest the pivotal role of Bcl-2 family members in the regulation of chondrocyte apoptosis.

Endochondral ossification is an essential process for skeletal development, fracture healing, and pathologic conditions such as osteoarthritis and ectopic ossification (1). In this process, chondrocytes first proliferate and then differentiate into mature hypertrophic chondrocytes, which mineralize the surrounding matrix that is finally replaced by bone (1). There is controversy as to the cell fate of hypertrophic chondrocytes, and several studies have shown that they undergo apoptosis after terminal differentiation (2–4). Apoptosis is a form of programmed cell death that is characterized by specific morphological and biochemical features, and is tightly regulated by extracellular stimuli and intracellular signaling pathways (5). Morphologically, apoptosis is characterized by a series of structural changes in dying cells as follows: blebbing of the plasma membrane, condensation of the cytoplasm and the nucleus, and cellular fragmentation into membrane apoptotic bodies. Biochemically, apoptosis is characterized by the degradation of chromatin, initially into large fragments of 50–300 kb and subsequently into smaller fragments that are monomers and multimers of 200 bases. Not only does apoptosis regulate various aspects of the biological activity, but it also can trigger cancer, autoimmune diseases, and degenerative disorders (6). Several molecules such as Sox5, -6, and -9 and Runx2 have been reported to regulate proliferation and hypertrophic differentiation of chondrocytes (7–9). However, the physiologic and pathologic significance of chondrocyte apoptosis and key molecules that regulate this process remain to be elucidated.

Previous studies have shown the possible involvement of cytokines, such as tumor necrosis factor-α and Fas ligand, and hormones, such as glucocorticoids and parathyroid hormone-related peptide (PTHrP),[2] in the localized hypoxia and increased generation of reactive oxygen species in chondrocyte apoptosis. Shapiro and co-workers (10–12) and Poole and co-workers (13) reported that the terminal differentiation of chondrocytes is accompanied by marked accumulation of extracellular phosphate ions, which may lead to chondrocyte apoptosis through a plasma membrane phosphate transporter mechanism. The importance of phosphate ions in chondrocyte apoptosis was also confirmed by Demay and co-workers (14), who reported that hypophosphatemia leads to impaired apoptosis of hypertrophic chondrocytes and subsequent expansion of the late hypertrophic chondrocyte layer in vitamin D receptor-null mice, which was reversed by feeding with a high phosphate diet. Although these reports indicate that P_i entry into the cells induces apoptosis in growth plate chondrocytes, the precise molecular mechanism that results in the apoptosis of chondrocytes is still an enigma.

* This work was authored, in whole or in part, by National Institutes of Health staff. This work was supported in part by grants-in-aid from the Ministry of Education, Culture, Sports, Science, and Technology of Japan and health science research grants from the Ministry of Health, Labor, and Welfare of Japan (to S. T.). The costs of publication of this article were defrayed in part by the payment of page charges. This article must therefore be hereby marked "*advertisement*" in accordance with 18 U.S.C. Section 1734 solely to indicate this fact.

[S] The on-line version of this article (available at http://www.jbc.org) contains supplemental Fig. 1.

[1] To whom correspondence should be addressed: Dept. of Orthopaedic Surgery, Faculty of Medicine, The University of Tokyo, Hongo7-3-1, Bunkyo-ku, Tokyo113-0033, Japan. Tel.: 81-3-3815-5415, ext. 33376; Fax: 81-3-3818-4082; E-mail: TANAKAS-ORT@h.u-tokyo.ac.jp.

[2] The abbreviations used are: PTHrP, parathyroid hormone-related peptide; RT, reverse transcription; cKO, conditional knock-out; RNAi, RNA interference; BH3, Bcr homology domain 3; Z, benzyloxycarbonyl; fmk, fluoromethyl ketone; LM, littermate; BH3, Bcl-2 homology 3.

There are two distinct signaling pathways of apoptosis in mammals. One is initiated by death receptors (death receptor pathways) (15), and the other is regulated by anti- and pro-apoptotic Bcl-2 family members and involves release of cytochrome *c* from mitochondria into the cytoplasm (mitochondrial pathways) (16, 17). The anti-apoptotic Bcl-2 family members include mammalian Bcl-2, Bcl-xL, and Mcl-1, and more than 20 pro-apoptotic Bcl-2 family proteins have been identified to date in mammals, which are divided into two groups as follows: multidomain members (Bax, Bak, Bok/Mtd, etc.) and BH3 domain-only members (Bid, Bad, Bim, Bik, Puma, Noxa, Bmf, Hrk, Bnip3, Nix, etc.) (18). Although the BH3-only family members display tissue-specific distribution patterns, multidomain pro-apoptotic members are ubiquitously expressed, indicating that BH3-only proteins play a tissue/cell-specific and a stimulus-specific role in apoptosis and that the other members play an essential role further downstream (18).

We report here that the balance between the anti-apoptotic Bcl-2 family member Bcl-xL and the pro-apoptotic family member Bnip3 critically regulates the apoptosis of terminally differentiated chondrocytes both *in vitro* and *in vivo*. We first showed that the Bcl-xL/Bnip3 axis plays an essential role in P_i-induced chondrocyte apoptosis *in vitro*. Subsequently, we generated mutant mice conditionally deficient in the *bcl-x* gene using the Cre-loxP recombination system, and we found that the hypertrophic chondrocyte layer was shortened in these mice because of increased apoptosis.

EXPERIMENTAL PROCEDURES

Plasmids and Viral Vectors—For the production of retrovirus, full-length cDNA of mouse *bcl-xL*, *bcl-2*, *mcl-1*, and *bnip3* was amplified by PCR, subcloned into pCR-TOPO II vectors (Invitrogen), and inserted into pMx vectors (19). The production of the retroviral vectors was performed as reported previously (20). Briefly, Plat-E cells (2×10^6 cells) were plated in 60-mm dishes and transfected with 2 μg of pMx vector using FuGENE (Roche Applied Science) on the following day. After 24 h, the medium was replaced with fresh medium, which was collected and used as the retroviral supernatant 48 h after the transfection. The puromycin-resistant gene and blasticidin-resistant gene were inserted into a pMx vector for the selection of stable cells. For gene silencing, RNAi sequences were designed for each of the mouse Bcl-2 family genes. Targeting sequences used were as follows: GCGTTCAGTGATCTAACATCC for Bcl-xL; GGATGCCTTTGTGGAACTATA for Bcl-2; GGACTGGCTTGTCAAACAAAG for Mcl-1; GGTAGGACAGAAACTAGAT for Bim; GGGTCAGCTATTATCTCAA for Bid; GAGCCAAACCTGACCACTA for Puma; GGTGGAGAGTTCAATTAAG for Bik; GAAGAGAAGTTGAAAGTAT for Bnip3; GGAAGAAAGTAAGTCTGAT for Nix; GGAAGGAAGCAGAATTGTA for Hrk; GCTCAAAGAAAGATGGCTT for Bmf; and GCTACGTCCAGGAGCGCACCA for green fluorescent protein. RNAi expression vectors for these genes were constructed with piGENEmU6 vector (for mouse) (iGENE Therapeutics) as described (21). For retrovirus expressing RNAi, the U6 promoter and inserts in piGENE vectors were cloned into pMx vectors. The adenovirus vector expressing $FADD^{DN}$, which lacks the N-terminal domain that is responsible for recruiting and activating caspase-8 at the death receptor complex (22), was created as described previously (7). Adenovirus vectors expressing bacterial Cre recombinase was a generous gift from Kojiro Ueki (University of Tokyo). Adenoviruses were amplified in HEK293 cells and purified with the AdenoX virus purification kit (Clontech). Viral titers were determined by the end point dilution assay, and the viruses were used at 50 multiplicities of infection.

DNA Transfection—For the gene transduction or knockdown of Bcl-2 family molecules, growth plate chondrocytes or ATDC5 cells (3×10^5 per well) were seeded onto 60-mm cell culture dishes. After 24 h, the cells were left untreated or treated with the retrovirus vectors together with Polybrene at 8 μg/ml. Thereafter, the medium was replaced with fresh medium containing 1 μg/ml of puromycin and/or 10 μg/ml of blasticidin until they became confluent. Selective overexpression or inhibition of Bcl-2 family member molecules was confirmed by real time RT-PCR or Western blotting.

Cell Culture—Growth plate chondrocytes were isolated from the ribs (excluding the sternum) of C57BL6 or $bcl\text{-}x^{fl/fl}$ mice embryos (E18.5). About 1×10^5 cells can be obtained from one mouse. They were cultured in high glucose Dulbecco's modified Eagle's medium (Sigma) containing 10% fetal bovine serum (Sigma) and 1% penicillin/streptomycin (Sigma). They are mainly composed of proliferating chondrocytes and were differentiated into hypertrophic chondrocytes and underwent apoptosis in the presence of P_i. Mouse chondrogenic ATDC5 cells were obtained from the RIKEN Cell Bank (Saitama, Japan). The cells were cultured in Dulbecco's modified Eagle's medium/F-12 (1:1) (Sigma) with 5% fetal bovine serum and 1% penicillin/streptomycin. To induce hypertrophic differentiation, ATDC5 cells were cultured in the presence of ITS supplement (10 μg/ml bovine insulin (I), 5.5 μg/ml human transferrin (T), and 5 ng/ml sodium selenite (S)) (Sigma) for 14 days. To induce apoptosis in ATDC5 cells, the medium was changed to α-minimum Eagle's medium, 5% fetal bovine serum supplemented with ascorbic acid 2-phosphate (0.05 mM) and phosphate (NaH_2PO_4) at concentrations of 0–20 mM for 24–48 h. These cells were maintained at 37 °C in a humidified 5% CO_2, 95% air atmosphere. The medium was replaced every other day.

Cell Viability Assay—Cell viability was determined by Cell Count Kit-8 (Dojindo) to count the living cells. Briefly, the cells were placed (1×10^5 cells per well) in a 96-well plate. After incubation with the indicated concentrations of P_i for 24 h, 10 μl of kit reagent was added and incubated for an additional 3 h. Cell viability was determined by scanning the samples with a microplate reader at 450 nm.

Western Blotting—Western blot analysis was performed with cell extracts from growth plate chondrocytes or ATDC5 cells. Cells were washed twice with ice-cold phosphate-buffered saline, and proteins were extracted with an M-PER, NE-PER (Pierce), or ApoAlert cell fractionation kit (Clontech), according to the manufacturer's instructions. Protein concentrations of the cell lysates were measured with a Protein Assay kit II (Bio-Rad). For Western blot analysis, lysates were fractionated by SDS-PAGE with 7.5–15% Tris-glycine gradient gel or 15% Tris-glycine gel and transferred onto nitrocellulose membranes (Bio-Rad). After blocking with 6% milk/TBS-T, membranes

were incubated with primary antibodies to Bcl-xL, Puma, Bik, Bid, cleaved caspase-3 and -7, cleaved lamin A (Cell Signaling Technology), Mcl-1, Hrk (Santa Cruz Biotechnology), Bcl-2, Bim (Pharmingen), Bnip3, Nix, Bmf, FLAG, β-actin (Sigma), cytochrome *c*, and Cox4 (Clontech), followed by horseradish peroxidase-conjugated goat anti-mouse IgG or goat anti-rabbit IgG (Promega). Immunoreactive bands were visualized with ECL Plus (Amersham Biosciences), according to the manufacturer's instructions. For co-immunoprecipitation, cells were lysed in 0.2% Nonidet P-40 isotonic buffer (0.2% Nonidet P-40, 142.5 mM KCl, 5 mM $MgCl_2$, 1 mM EGTA, 20 mM HEPES, pH 7.5). Cell lysates were immunoprecipitated with anti-Bcl-xL antibody (Cell Signaling Technology) and separated by SDS-PAGE with a 15% Tris-glycine gradient gel.

Real Time Quantitative RT-PCR—Total RNA was extracted with ISOGEN (Wako Pure Chemicals Industries, Ltd.), and an aliquot (1 μg) was reverse-transcribed using a Takara RNA PCR kit (avian myeloblastosis virus) version 2.1 (Takara Shuzo Co., Ltd.) to make single-stranded cDNA. PCR was performed on an ABI Prism 7000 sequence detection system (Applied Biosystems Inc.) using QuantiTect SYBR Green PCR Master Mix (Qiagen) according to the manufacturer's instructions. After data collection by the ABI Prism 7000 sequence detection system, the mRNA copy number of a specific gene in the total RNA was calculated, and a standard curve generated with serially diluted plasmids containing PCR amplicon sequences, and normalized to rodent total RNA (Applied Biosystems) with mouse β-actin as an internal control. Standard plasmids were synthesized with a TOPO TA cloning kit (Invitrogen), according to the manufacturer's instruction.

Primer Information—Each primer sequence of mouse target genes is described as follows: 5'-TGCAGAGGATGATTGCTGAC-3' and 5'-GATCAGCTCGGGCACTTTAG-3' for Bax; 5'-AGGTGACAAGTGACGGTGGT-3' and 5'-AAGATGCTGTTGGGTTCCAG-3' for Bak; 5'-ACATGGGGCAAGGTAGTGTC-3' and 5'-GCTGACCACACACTTGAGGA-3' for Bok; 5'-TTCGGTGTGATGTACCTGGA-3' and 5'-CCAGGATGTTGTCACTGTCG-3' for Bcl-Rambo; 5'-CAGACCCTCAGTCCAGCTTC-3' and 5'-CGTATGAAGCCGATGGAACT-3' for Bmf; 5'-ACAACCGCGAGCCAGGTA-3' and 5'-CAGGGCATAGAACTCGGAAG-3' for Bcl2l12; 5'-CGGGCAGAGCTACCACCT-3' and 5'-CGAGCGTTTCTCTCATCACA-3' for Noxa; 5'-CTCAGCTTGGCAGAACACAT-3' and 5'-GCAGACACAGGTCCATCTCA-3' for Bik; 5'-GCCCAGACATTTGGTCAGTT-3' and 5'-TGCACACACACACAGAGGAA-3' for Bim; 5'-CGAGCAACAGGTTAGCGAAA-3' and 5'-TGCACAGGTACGGAATTTTG-3' for Hrk; 5'-CCACAGCTCTCAGTCAGAAGAA-3' and 5'-GTGTGCTCAGTCGTTTTCCA-3' for Nix; 5'-GCCCAGCAGCACTTAGAGTC-3' and 5'-TGTCGATGCTGCTCTTCTTG-3' for Puma; 5'-GCTTGGGGATCTACATTGGA-3' and 5'-TCAGGAACACCGCATTTACA-3' for Bnip3; 5'-CTCTGCGTTCAGCTTGAGTG-3' and 5'-CAGAAGCCCACCTACATGGT-3' for Bid; 5'-AGGGATGGAGGAGGAGCTTA-3' and 5'-TAGAGTTCCGGGATGTGGAG-3' for Bad; 5'-GCCAAGACCTGAAACTCTGC-3'; and 5'-GCCATAGCTGAAGTGGAAGC-3' for col2; 5'-CATAAAGGGCCCACTTGCTA-3' and 5'-TGGCTGATATTCCTGGTGGT-3' for col10; 5'-AGATGTGGATCAGCAAGCAG-3'; and 5'-GCGCAAGTTAGGTTTTGTCA-3' for β-actin.

Mice—Mice carrying the *bcl-x* gene with two loxP sequences at the promoter region and the second intron (*bcl-x*$^{fl/fl}$ mice) were generated as reported previously (23). The mice are on a 129SvEv and C57BL6 mixed background. The presence of the floxed *bcl-x* gene was determined by PCR around the 5' loxP site using the primers 5'-CGG TTGCCT AGC AAC GGG GC-3' and 5'-CTC CCA CAG TGG AGA CCTCG-3', giving a wild-type band of 200 bp and a floxed gene product of 300 bp. These *bcl-x*$^{fl/fl}$ mice have been used successfully to examine the role of Bcl-xL in a variety of cell types, including those in the liver, ovary, mammary gland, and substantia nigra, as well as in erythroid cells and dendritic cells (23–28). To generate chondrocyte-specific *bcl-x* knock-out mice, *bcl-x*$^{fl/fl}$ mice were crossed with type II collagen (Col2a1)-Cre transgenic mice, which express the Cre recombinase gene under the control of the *col2a1* gene promoter (29). Col2a1-Cre$^{+/-}$ *bcl-x*$^{fl/fl}$ (cKO), and Col2a1-Cre$^{-/-}$ *bcl-x*$^{fl/fl}$ (normal littermates) mice were generated by mating Col2a1-Cre$^{+/-}$ *bcl-x*$^{fl/+}$ male mice with Col2a1-Cre$^{-/-}$ *bcl-x*$^{fl/fl}$ female mice. All animals were housed under specific pathogen-free conditions and treated with humane care under approval from the Animal Care and Use Committee of the University of Tokyo.

Histological Analysis—Tissues were fixed in 4% paraformaldehyde/phosphate-buffered saline, decalcified in 10% EDTA, embedded in paraffin, and cut into sections of 5-μm thickness. Hematoxylin and eosin staining as well as von Kossa staining were performed according to the standard procedure. For immunohistochemistry, sections were incubated overnight at 4 °C with primary antibodies against Bcl-xL (1:200; Cell Signaling Technology), Bnip3 (1:200; Sigma), COL10 (1:500; LSL) and cleaved caspase-7 (1:100; Cell Signaling Technology). The localization of the antigens was visualized by incubation with horseradish peroxidase-conjugated secondary antibodies (Promega) followed by incubation with 3,3'-diaminobenzidine according to the manufacturer's protocol. For fluorescent visualization, a secondary antibody conjugated with Alexa 488 (Molecular Probes) was used. A bone radiograph of whole bodies, femurs, and tibiae was taken with a soft x-ray apparatus (SOFTEX, CMB-2, Tokyo, Japan).

Statistical Analysis—Statistical analyses were performed using two-tailed unpaired Student's *t* test for the real time PCR and cell viability assay. A p value of <0.05 was considered to be statistically significant. The results are presented as means ± S.D.

RESULTS

P_i Induces Apoptosis of Chondrocytes through Mitochondrial Pathways—We first evaluated the effect of P_i on the viability of primary chondrocytes *in vitro*. When mouse primary chondrocytes were stimulated with P_i, a dose- and time-dependent increase in cell death was observed (Fig. 1*A*). Only about 40% of the chondrocytes survived 24 h after stimulation with 20 mM P_i. Phosphonoformic acid, which inhibits P_i entry into the cells, almost completely restored P_i-induced cell death, as reported previously (data not shown), indicating that the intracellular P_i transport stimulated chondrocyte cell death. In addition,

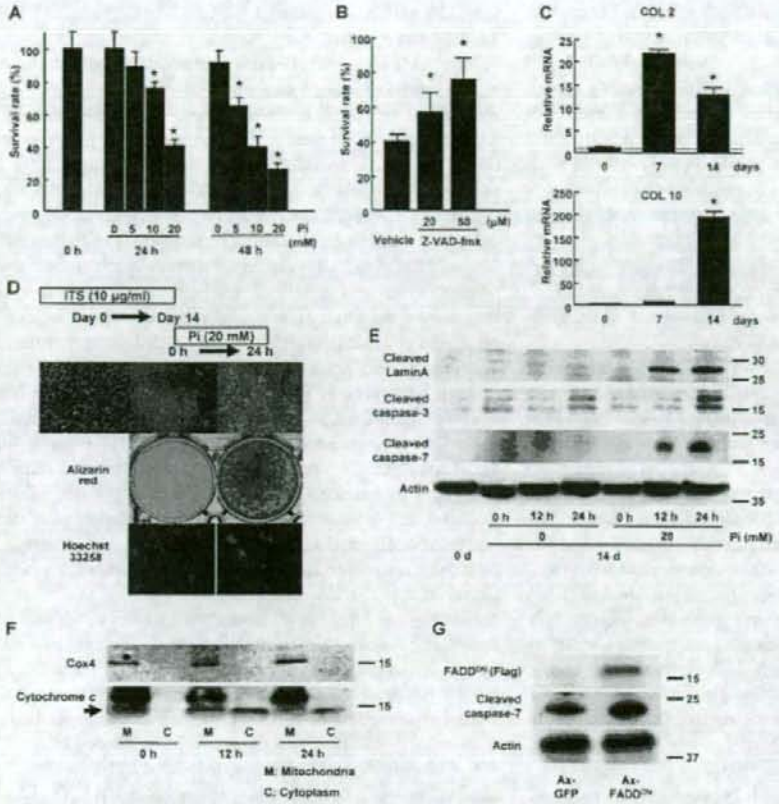

FIGURE 1. **P_i-induced chondrocyte apoptosis.** *A*, P_i-induced cell death of primary chondrocytes in a dose- and time-dependent manner. The results are expressed as the means ± S.D. of six cultures. Experiments were repeated at least three times, and the representative data are presented. *, significantly different from untreated group, $p < 0.05$. *B*, pan-caspase inhibitor Z-VAD-fmk dose-dependently inhibited P_i-induced cell death of primary chondrocytes. The cells were treated with either vehicle or Z-VAD-fmk for 30 min before P_i stimulation (20 mM). The results are expressed as the means ± S.D. of six cultures. Experiments were repeated at least three times, and the representative data are presented. *, significantly different from vehicle-treated group, $p < 0.01$. *C*, expression of type II (*Col 2*) and type X collagen (*Col 10*) expression in ITS-treated ATDC5 cells as determined by real time PCR. Type II collagen expression was increased by day 7 of ITS treatment, which was followed by an increase in a hypertrophic chondrocyte marker, type X collagen. The results are expressed as the means ± S.D. of three samples. Experiments were repeated at least three times, and the representative data are presented. *, significantly different from day 0, $p < 0.01$. *D*, P_i stimulation induced the mineralization and apoptosis of differentiated ATDC5 cells. ATDC5 cells exhibited nodule formation when treated with ITS for 14 days, whereas neither mineralization (*middle panel*) nor chromatin condensation (*bottom panel*) was observed in the absence of P_i treatment. P_i stimulation (20 mM) of the cells rapidly induced mineralization of the surrounding matrix and the nuclear condensation characteristic of apoptotic cells. *E*, Western blot analysis of ATDC5 cells. P_i stimulation at 20 mM after ITS treatment for 14 days induced caspase 3 and 7 activation and Lamin proteolysis in ATDC5 cells in the 12–24-h period. *F*, subcellular fractionation of ATDC5 cells. Cytochrome *c*, which was exclusively localized in mitochondrial fraction (*M*), was released into the cytoplasmic fraction (*C*) in response to P_i stimulation (*arrow*). Cox4 is a marker of the mitochondrial fraction. Upper bands in mitochondrial fraction are nonspecific bands. *G*, overexpression of $FADD^{DN}$ did not affect P_i-induced caspase 7 activation of ATDC5 cells, which were pretreated with ITS for 14 days. Adenovirus of green fluorescent protein GFP or $FADD^{DN}$ was introduced 48 h before P_i stimulation (20 mM).

administration of the caspase inhibitor Z-VAD-fmk dose-dependently blocked cell death (Fig. 1*B*), indicating that P_i-induced cell death is a caspase-dependent process, *i.e.* apoptosis.

Next, we investigated the molecular mechanisms that lead to hypertrophic differentiation, mineralization, and apoptosis of chondrocytes, using a chondrogenic cell line, ATDC5. ATDC5 cells express markers of hypertrophic chondrocytes and mineralize the surrounding matrix under ITS treatment and subsequent P_i stimulation (30, 31). During ITS treatment, the expression of a chondrocyte marker type II collagen increased earlier than day 7 and remained high levels on day 14. In contrast, the expression of a hypertrophic chondrocyte marker type X collagen was low on day 7, and gradually increased thereafter, and was highly expressed on day 14 (Fig. 1*C*). Neither mineralization nor caspase activation was observed (Fig. 1*D*). After P_i stimulation, the cells underwent mineralization and apoptosis within 24 h (Fig. 1*E*). To examine the localization of cytochrome *c* in the course of the apoptosis of ATDC5 cells, we performed cell fractionation experiments. Cytochrome *c* was mainly detected in the mitochondrial fractions, which is positive for Cox4, before P_i stimulation, and was released into the cytoplasm in response to P_i stimulation (Fig. 1*F*). The differentiation and apoptosis of chondrocytes are independently regulated since overexpression of *runx2* or dominant negative *runx2* did not affect Pi-induced apoptosis. Adenovirus vector-mediated introduction of dominant negative FADD ($FADD^{DN}$), which blocks death receptor-initiated apoptosis, almost completely abolished tumor necrosis factor-α-induced cell death (data not shown) but did not affect P_i-induced apoptosis in ATDC5 cells (Fig. 1*G*). These results suggest that the mitochondrial pathway, but not the death receptor pathway, is mainly involved in the P_i-induced apoptosis of ATDC5 cells.

Bcl-xL Regulates Chondrocyte Apoptosis—Because mitochondrial pathways are primarily regulated by Bcl-2 family member proteins, we next examined the expression levels and functions of Bcl-2 family molecules during the differentiation and apoptosis of chondrocytes. We first examined the effect of gain or loss of function of anti-apoptotic Bcl-2 family members, Bcl-2, Bcl-xL, and Mcl-1, on the cell viability of ATDC5 cells. Among these three molecules, Bcl-xL most efficiently suppressed P_i-induced chondrocyte apoptosis when overexpressed by retroviral vectors (Fig. 2*A*). Conversely, the knockdown of *bcl-xL* gene through RNAi efficiently reduced the cell viability compared with the knockdown of the *bcl-2* or *mcl-1* gene (Fig.

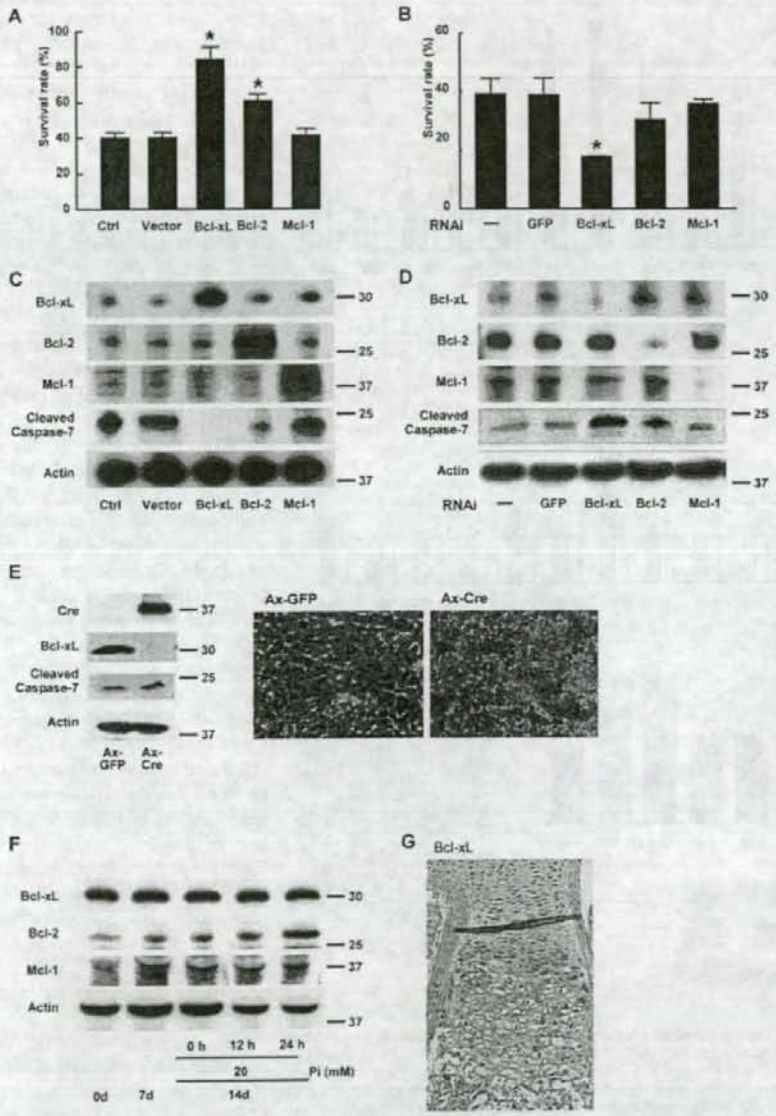

FIGURE 2. **Role of anti-apoptotic Bcl-2 family member proteins in P_i-induced apoptosis (20 mM).** *A* and *B*, effects of anti-apoptotic Bcl-2 family member proteins on P_i-induced apoptosis of primary chondrocytes. Overexpression of Bcl-xL and Bcl-2 significantly suppressed the P_i-induced cell death of primary chondrocytes (*A*), whereas gene silencing of Bcl-xL alone promoted it (*B*). The results are expressed as the means ± S.D. of six cultures. *Ctrl*, control; *GFP*, green fluorescent protein. *C* and *D*, effects of anti-apoptotic Bcl-2 family proteins on caspase activation in ATDC5 cells after P_i stimulation as determined by Western blot analysis. P_i-induced caspase-7 activation as determined by cleave caspase-7 blotting was most efficiently suppressed by Bcl-xL transduction. Bcl-2 transduction had a milder activity, and Mcl-1 transduction had no effect (*C*). Gene silencing of Bcl-xL markedly increased P_i-induced caspase-7 activation, whereas that of Bcl-2 had milder effect, and Mcl-2 had no effect (*D*). Mcl-2 was detected as diffuse bands. *E*, adenovirus vector-mediated overexpression of Cre recombinase efficiently down-regulated *bcl-x* gene in primary chondrocytes obtained from *bcl-x*$^{fl/fl}$ mice and induced caspase-7 activation (*left*) in the cells, and they underwent morphological apoptosis (*right*). *F*, expression levels of anti-apoptotic Bcl-2 family member proteins in ATDC5 cells during ITS treatment and P_i stimulation. No significant change was observed. *G*, immunohistological examination of a murine metatarsal bone (E18.5) with anti-Bcl-xL antibody. Bcl-xL was uniformly expressed in the growth plate chondrocytes.

2*B*). Western blot analysis revealed that cleaved caspase-7 expression was suppressed by Bcl-xL overexpression and increased by its knockdown in differentiated ATDC5 cells treated with P_i (Fig. 2, *C* and *D*). The important role of Bcl-xL was further confirmed by the experiments using primary chondrocytes obtained from *bcl-x*$^{fl/fl}$ mice. Adenovirus vector-mediated overexpression of Cre recombinase efficiently down-regulated *bcl-x* gene in primary chondrocytes obtained from *bcl-x*$^{fl/fl}$ mice and induced caspase-7 activation (Fig. 2*E*, *left*) in the cells, and they became apoptotic morphologically (Fig. 2*E*, *right*). These results suggest that Bcl-xL primarily maintains the viability of chondrocytes. However, the expression levels of Bcl-xL did not appear to change in the course of chondrocytic differentiation or P_i-induced apoptosis in ATDC5 cells (Fig. 2*F*). In addition, immunohistological examination revealed that Bcl-xL is uniformly expressed in growth plate chondrocytes (Fig. 2*G*). It should be noted that the expression of another anti-apoptotic member Bcl-2 increased in response to P_i stimulation, suggesting an important role of the molecule in regulating chondrocyte apoptosis (Fig. 2*F*). However, the increased level of Bcl-2 was not enough to suppress P_i-induced apoptosis of ATDC5 cell.

Bnip3, a Pro-apoptotic Bcl-2 Family Member Protein, Promotes the P_i-induced Apoptosis of Chondrocytes—The fact that the expression level of Bcl-xL was not affected by P_i stimulation and that Bcl-xL is uniformly expressed in the chondrocyte layers prompted us to investigate the role of pro-apoptotic molecule(s) that may inhibit the anti-apoptotic function of Bcl-xL. Among 15 pro-apoptotic Bcl-2 family members, six molecules (Puma, Bid, Hrk, Bnip3, Bad, and Nix) increased in expression level during the course of hypertrophic differentiation (Fig. 3*A*), and two of them (Bnip3 and Bmf) in response to P_i stimulation (Fig. 3*B*). As shown in Fig. 3*C*, gene silencing of the pro-

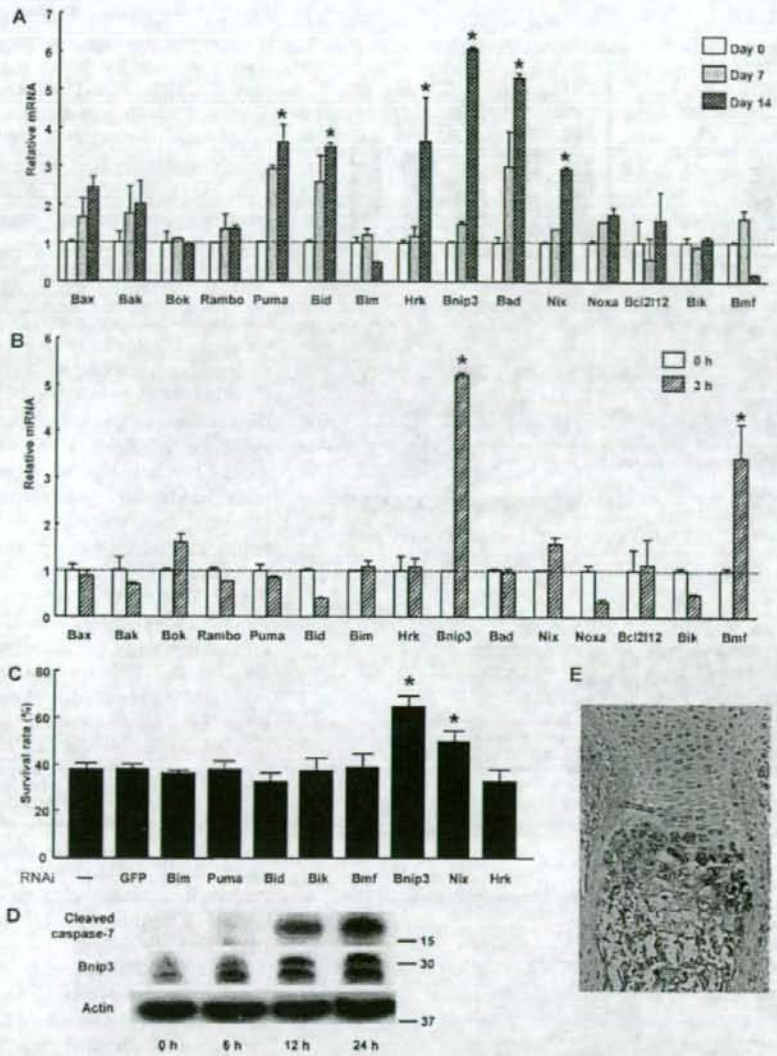

FIGURE 3. **Role of pro-apoptotic Bcl-2 family member proteins in P_i-induced cell death.** *A*, expression patterns of pro-apoptotic Bcl-2 family member proteins in ATDC5 cells during ITS treatment as determined by time and RT-PCR. The results are expressed as the means ± S.D. of three cultures. Experiments were repeated at least three times, and the representative data are presented. *, significantly different from day 0, $p < 0.05$. *B*, expression patterns of pro-apoptotic Bcl-2 family member proteins in ATDC5 cells after P_i stimulation as determined by real time PCR. ATDC5 cells were pretreated with ITS for 14 days (0 h) before P_i stimulation (20 mM). The results are expressed as the means ± S.D. of three cultures. Experiments were repeated at least three times, and the representative data are presented. *, significantly different from time 0, $p < 0.05$. *C*, effect of gene silencing of pro-apoptotic Bcl-2 family member proteins on cell viability of primary chondrocytes 24 h after P_i stimulation. Gene silencing of Bnip3 and Nix significantly promoted the cell viability, $p < 0.05$. The results are expressed as the means ± S.D. of six cultures. Experiments were repeated at least three times, and the representative data are presented. *GFP*, green fluorescent protein. *D*, Western blot analysis after P_i stimulation. Protein levels of Bnip3 increased in ATDC5 cells after 6 h of P_i stimulation, which was followed by caspase-7 activation. Bnip3 was detected as two bands. *E*, immunohistological examination of a murine metatarsal bone (E18.5) with anti-Bnip3 antibody. Bnip3 expression was primarily localized in the hypertrophic layers of chondrocytes.

apoptotic BH3-only molecule *bnip3* significantly suppressed P_i-induced apoptosis. Western blot analysis revealed that the protein levels of Bnip3 increased in response to P_i stimulation, followed by caspase-7 activation (Fig. 3*D*). Immunohistological examination of murine growth plates revealed that Bnip3 expression was exclusively localized in the prehypertrophic and hypertrophic layers of chondrocytes (Fig. 3*E*). Although overexpression of Bnip3 increased P_i-induced chondrocyte apoptosis, its overexpression alone failed to induce chondrocyte apoptosis in the absence of P_i (data not shown).

Bnip3 Associates with Bcl-xL and Attenuates the Anti-apoptotic Effect of Bcl-xL on Chondrocytes—We then investigated the molecular interaction between Bcl-xL and Bnip3 in chondrocytes. Earlier studies have shown that Bnip3 heterodimerizes with Bcl-2 and Bcl-xL and facilitates cell death via mitochondrial pathways (32). As shown in Fig. 4*A*, Bnip3 was co-immunoprecipitated with Bcl-xL in P_i-treated chondrocytes. The susceptibility to apoptosis by *bcl-xL* knockdown was partially restored by simultaneous silencing of *bnip3* (Fig. 4*B*). Conversely, overexpression of Bnip3 promoted P_i-induced cell death, which was almost completely rescued by the simultaneous transduction of Bcl-xL but not by that of Bcl-2 or Mcl-1 (Fig. 4*C*). Taken together, Bnip3 is up-regulated and associates with Bcl-xL in chondrocytes in response to P_i stimulation, impairs the anti-apoptotic function of Bcl-xL, and consequently causes apoptosis in these cells.

Chondrocyte-specific Bcl-x Knockout Mice Exhibit a Reduction in the Hypertrophic Layer of Growth Plate Chondrocytes—To further confirm the essential role of the Bcl-xL/Bnip3 axis in chondrocytes, we generated chondrocyte-specific conditional knock-out (cKO) mice of the *bcl-x* gene by mating *bcl-x*$^{fl/fl}$ mice with Col2a1-Cre transgenic mice, in which Cre recombinase is specifically expressed in chondrocytes under the control of the *col2a1* promoter. The cKO mice (Col2a1-Cre$^{+/-}$ *bcl-x*$^{fl/fl}$ mice) were born at approximately a Mendelian frequency. Bcl-xL expression was markedly reduced in chondrocytes of the cKO mice,

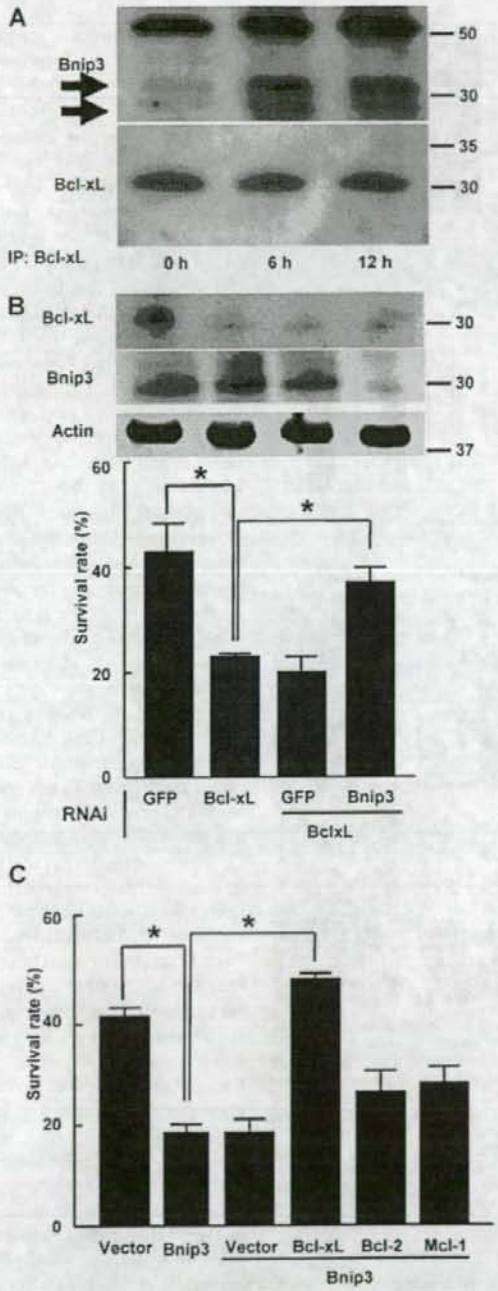

FIGURE 4. **Molecular interaction between Bcl-xL and Bnip3 in chondrocytes.** *A*, Bcl-xL was immunoprecipitated (*IP*) from ATDC5 cells left untreated or treated with 20 mM P_i. The immunoprecipitated materials were Western blotted with anti-Bnip3 antibody. Bnip3 was associated with Bcl-xL after 6 h of P_i treatment. Bnip3 was detected as two bands (*arrows*). The top band is the immunoglobulin heavy chain. *B*, susceptibility to apoptosis of primary chondrocytes by Bcl-xL knockdown was partially restored by the simultaneous silencing of Bnip3. Western blot analysis shows efficient gene knockdown of Bcl-xL and Bnip3 through RNAi. The results are expressed as the means ± S.D. of six cultures. Experiments were repeated at least three times, and the representative data are presented. *, significantly different, $p < 0.05$. *GFP*, green fluorescent protein. *C*, overexpression of Bnip3 promoted the P_i-induced cell death of primary chondrocytes, which was rescued by simultaneous transduction of Bcl-xL, whereas overexpression of Bcl-2 or Mcl-1 had little effect. The results are expressed as the means ± S.D. of six cultures. Experiments were repeated at least three times and the representative data are presented. *, significantly different, $p < 0.05$.

whereas its expression in other cells or tissues was comparable with that in their normal littermates (LM) that did not carry the *col2a1-cre* gene (Col2a1-Cre$^{+/-}$ *bcl-x*$^{fl/fl}$ mice) (Fig. 5*A*). *bcl-x* cKO mice exhibited dwarfism, with shortened limbs and trunk compared with their normal littermates (*bcl-x*$^{fl/fl}$ mice) (Fig. 5*B*). The trunk of the cKO mice was about 10% shorter than that of *bcl-x*$^{fl/fl}$ mice at 5 weeks of age. The longitudinal length of the femur and tibia, which are formed through endochondral ossification, were also significantly shorter in cKO mice (Fig. 5, *C* and *D*). Histological analysis of the growth plates of the proximal tibia showed that the hypertrophic chondrocyte layer was markedly shortened in cKO mice, probably because of an increased apoptosis of prehypertrophic and hypertrophic chondrocytes, as determined by immunohistochemical analysis of cleaved caspase-7 (Fig. 5*E*). No abnormality in vascular invasion was observed (data not shown). Bnip3 was predominantly expressed in the prehypertrophic and hypertrophic layers of chondrocytes, and its expression level was not different between the cKO mice and their normal littermates. Taking these histological findings together, Bcl-xL is essential for the survival of prehypertrophic and hypertrophic chondrocytes by antagonizing the pro-apoptotic function of Bnip3.

DISCUSSION

Although the molecular mechanism and pathophysiologic role of chondrocyte apoptosis have not been fully elucidated yet, the possible involvement of P_i in this process has been suggested. It was reported that both intracellular and extracellular calcium and phosphate levels increase in the hypertrophic area where terminally differentiated chondrocytes mineralize the surrounding matrix and subsequently die (11, 30, 33). *In vitro* studies have also made clear that P_i induces the mineralization and cell death of chondrocytes (11, 12). Magne *et al.* (30) thoroughly investigated the involvement of P_i and Ca^{2+} in chondrocyte maturation using ATDC5 cells, and showed that P_i is a key regulator of chondrocyte maturation, mineralization, and apoptosis. In addition, disorders in P_i homeostasis result in abnormal endochondral ossification, and hypophosphatemia caused by inefficient phosphate reabsorption by the kidney is associated with defective mineralization of the skeleton, which manifests as rickets or osteomalacia (34, 35). Sabbagh *et al.* (14) reported that hypophosphatemia, but not hypocalcemia or hyperparathyroidism, is responsible for the reduced chondrocyte apoptosis and the subsequent rachitic changes in vitamin D receptor-null mice and Hyp mice. All of these observations indicate a crucial role of P_i in controlling the cell fate of hypertrophic chondrocytes.

This study shows that hypertrophic chondrocytes are susceptible to P_i-induced apoptosis, which is regulated by the bal-

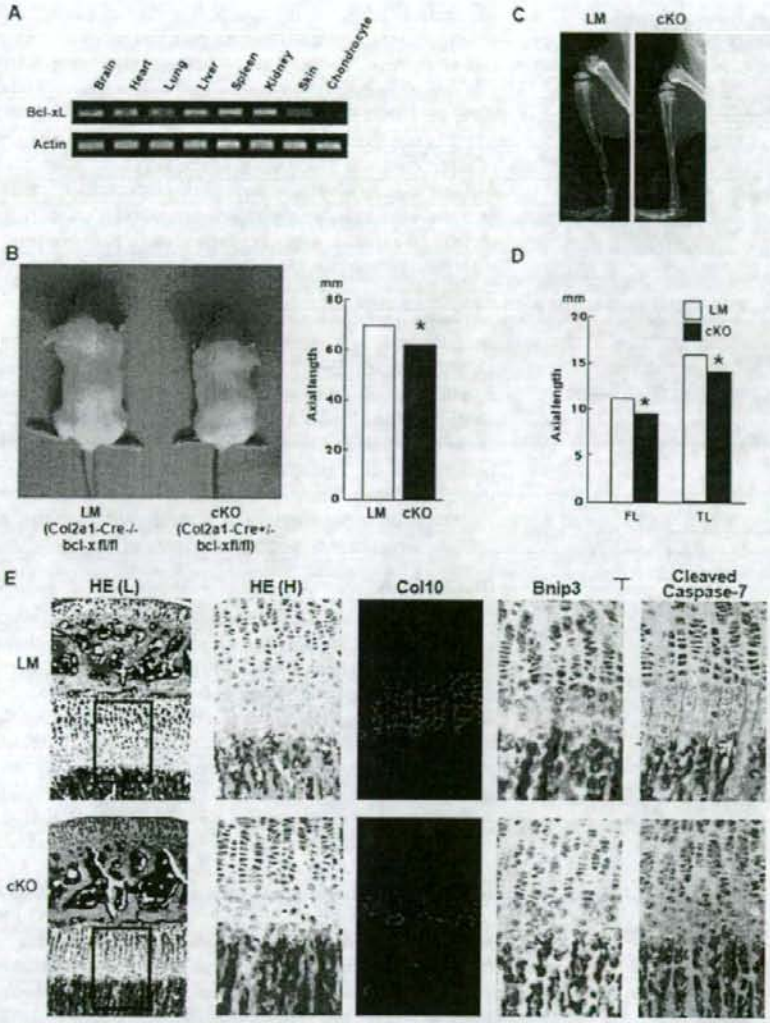

FIGURE 5. **Chondrocyte-specific *bcl-x* knock-out mice.** *A*, RT-PCR of Bcl-xL expression. Bcl-xL expression was specifically reduced in chondrocytes. *B*, gross appearance of a chondrocyte-specific *bcl-x*-deficient mouse (*cKO*) and a normal littermate (*LM*) at 5 weeks of age (*left panel*). Total axial length (from the nose to the tail end) of cKO mice was significantly reduced in cKO mice, $p < 0.05$. The results are expressed as the means ± S.D. of three samples. *C*, representative x-ray images of hind limbs of LM and cKO mice at 5 weeks of age. The total bone length of the tibia as well as the growth plate length of cKO mice was shorter than that of their normal littermates. *D*, bone lengths of LM and cKO mice at 5 weeks of age. *FL*, femoral length; *TL*, tibial length. The results are expressed as the means ± S.D. of three samples. *, significantly different, $p < 0.05$. *E*, histological analysis of the growth plates of the proximal tibia at 5 weeks of age. In cKO mice, the hypertrophic layers, as evidenced by type X collagen staining, were shorter than those in LM mice. Although Bnip3 expression levels showed no difference between LM and cKO mice, the number of cleaved caspase-7-positive cells in the pre-hypertrophic and hypertrophic area was increased in cKO mice. *HE*, hematoxylin and eosin staining. *HE(H)* is the higher magnification of the rectangular areas in *HE(L)*.

ance maintained between pro-apoptotic and anti-apoptotic Bcl-2 family members. Among the anti-apoptotic members of the Bcl-2 family, overexpression of an anti-apoptotic member Bcl-xL suppressed and, conversely, its down-regulation by RNAi stimulated P_i-induced chondrocyte apoptosis most efficiently. Although overexpression of Bcl-2 also suppressed chondrocyte apoptosis, its suppression by RNAi was not as efficient as Bcl-xL knockdown was in inducing chondrocyte apoptosis. In addition, although Bcl-2-deficient mice exhibit abnormal skeletal development because of the accelerated maturation of chondrocytes (36), no apparent increase in chondrocyte apoptosis was observed in these mice (data not shown). Overexpression or down-regulation of Mcl-1 did not affect P_i-induced chondrocyte apoptosis. These results suggest that Bcl-xL is mainly implicated in the survival of chondrocytes, although it is also likely that other anti-apoptotic Bcl-2 family members have additive or synergistic roles with Bcl-xL. Because the skeletal phenotypes of *bcl-x* gene knock-out mice have not been investigated because of their embryonic lethality, we generated chondrocyte-specific *bcl-x* gene knock-out mice using the Cre-loxP recombination system. The mice exhibited dwarfism and immunohistological examination of the growth plate revealed a shortening of the hypertrophic layer because of the massive apoptosis of hypertrophic chondrocytes, confirming the pivotal role of Bcl-xL in hypertrophic chondrocyte survival. Amizuka *et al.* (37) previously reported that the apoptosis of chondrocytes was increased in the hypertrophic zone of PTHrP-deficient mice. Park *et al.* (38) recently reported that the transcriptional repressor Nkx3.2/Bapx1, which acts downstream of parathyroid hormone/PTHrP receptor signaling, enhances chondrocyte survival by constitutively activating RelA in a ligand-independent manner. However, because the morphological features of growth plates of *bcl-x* cKO mice were quite different from those of PTHrP-deficient mice, in which the number of proliferating chondrocytes was markedly reduced because of apoptosis and accelerated endochondral ossification was observed, we speculated that the apoptosis of hypertrophic chondrocytes in *bcl-x* cKO mice is not because of a defect in the PTHrP receptor/Nkx3.2 axis. Colnot *et al.* (39) demonstrated that anti-apoptotic protein Galectin 3 regulates the survival of chondrocytes, and its deficiency in mice results in

an accumulation of empty lacuna at the junction between avascular cartilage and vascular bone, without affecting endochondral ossification. From these results, they concluded that the apoptosis of hypertrophic chondrocytes does not affect the longitudinal bone growth. In contrast, *bcl-x* cKO mice displayed a dwarf phenotype, which was considered to be caused by the increased apoptosis of hypertrophic chondrocytes. The reason for the discrepancy between their results and ours remains elusive, and further investigation will be required to clarify the relationship between Bcl-xL and Galectin 3.

Because the expression levels of Bcl-xL and other anti-apoptotic members did not appear to change in the course of the hypertrophic differentiation and the apoptosis of chondrocytes, we speculated that the expression of pro-apoptotic molecule(s) is up-regulated in the hypertrophic chondrocytes and impairs the anti-apoptotic effect of Bcl-xL. By screening the pro-apoptotic Bcl-2 family members, we identified Bnip3 as a putative candidate pro-apoptotic gene in chondrocytes. Bnip3 belongs to the BH3-only subgroup members and facilitates both caspase-dependent and -independent apoptosis by antagonizing Bcl-2 or Bcl-xL activity (32, 40). Bnip3 is ubiquitously expressed, and its expression levels change in a number of tumors (35, 41). Interestingly, it was reported that the interaction between Bnip3 and Bcl-xL, and indeed the ability of BNIP3 to induce apoptosis, does not depend on the presence of a BH3 domain in BNIP3. Bnip3 is also involved in ischemia-induced cardiac myocyte cell death by acting downstream of the transcriptional hypoxia-inducible factor 1a (HIF-1a) (42). We found that the expression of Bnip3 increased in accordance with hypertrophic differentiation and during P_i-induced apoptosis in ATDC5 cells, which corresponded to the expression patterns of Bnip3 in the growth plate, as demonstrated by immunohistological examinations. Bnip3 increases its expression levels in response to P_i stimulation and binds to Bcl-xL in P_i-treated chondrocytes. In addition, knockdown of Bnip3 blocked P_i-induced apoptosis of chondrocytes, and therefore we concluded that Bnip3 determines the cell fate of hypertrophic chondrocytes by impairing the anti-apoptotic function of Bcl-xL, although the involvement of other BH3-only proteins cannot be completely excluded. Overexpression of Bnip3 increased P_i-induced chondrocyte apoptosis but failed to induce apoptosis in the absence of P_i (data not shown), indicating that other molecules induced by P_i stimulation is also required for chondrocyte apoptosis. Previous reports have shown an increase in HIF-1a levels in hypertrophic chondrocytes (43), which may stimulate Bnip3 expression.

Because P_i accelerates the terminal differentiation of chondrocytes, as evidenced by increased expression levels of type X collagen, it is possible that P_i induces chondrocyte apoptosis by simply accelerating terminal differentiation of the cells. However, overexpression of Bnip3 induced the apoptosis of chondrocytes without affecting their hypertrophic differentiation, indicating that the differentiation and the apoptosis of chondrocytes are distinctly regulated. While we were preparing the manuscript, Diwan *et al.* (44) recently reported the phenotype of Bnip3 knock-out mice with no increase in mortality or apparent physical abnormalities. Detailed analysis of the growth plates is necessary to clarify whether there is any abnormality in chondrocyte phenotypes in the KO mice, and whether Bnip3 functions as a *bona fide* BH3-only protein in chondrocytes remains to be determined.

Recently, Bnip3 has been reported to be involved in autophagy in hypoxic cardiac cells (42). Autophagy is primarily considered a pro-survival rather than pro-death mechanism. However, recent studies have revealed that it is also linked to programmed cell death, which is inhibited by Bcl-xL (45). Moreover, terminally differentiated chondrocytes are reported to exhibit autophagic characteristics (46). Because growth plate chondrocytes are exposed to hypoxic stress (43), autophagy may emerge to help survive such conditions. Although the precise mechanism of autophagic cell death remains unclear, the apoptotic cell death and the autophagic cell death might be intricately intertwined with each other in growth plate chondrocytes and regulated by Bcl-xL and Bnip3.

In summary, the apoptosis of hypertrophic chondrocytes is at least partly regulated by the balance between anti-apoptotic Bcl-xL and pro-apoptotic Bnip3, in which P_i appears to play a critical role. Further studies will be required to fully detail the molecular events regulating chondrocyte apoptosis, which have begun to be uncovered here.

Acknowledgment—We thank R. Yamaguchi (Dept. of Orthopaedic Surgery, University of Tokyo) who provided expert technical assistance. Pacific Edit reviewed the manuscript prior to submission.

REFERENCES

1. Kronenberg, H. M. (2003) *Nature* **423,** 332–336
2. Farnum, C. E., and Wilsman, N. J. (1987) *Anat. Rec.* **219,** 221–232
3. Gibson, G. J., Kohler, W. J., and Schaffler, M. B. (1995) *Dev. Dyn.* **203,** 468–476
4. Hatori, M., Klatte, K. J., Teixeira, C. C., and Shapiro, I. M. (1995) *J. Bone Miner. Res.* **10,** 1960–1968
5. Kerr, J. F., Wyllie, A. H., and Currie, A. R. (1972) *Br. J. Cancer* **26,** 239–257
6. Thompson, C. B. (1995) *Science* **267,** 1456–1462
7. Ikeda, T., Kamekura, S., Mabuchi, A., Kou, I., Seki, S., Takato, T., Nakamura, K., Kawaguchi, H., Ikegawa, S., and Chung, U. I. (2004) *Arthritis Rheum.* **50,** 3561–3573
8. Inada, M., Yasui, T., Nomura, S., Miyake, S., Deguchi, K., Himeno, M., Sato, M., Yamagiwa, H., Kimura, T., Yasui, N., Ochi, T., Endo, N., Kitamura, Y., Kishimoto, T., and Komori, T. (1999) *Dev. Dyn.* **214,** 279–290
9. Yoshida, C. A., Yamamoto, H., Fujita, T., Furuichi, T., Ito, K., Inoue, K., Yamana, K., Zanma, A., Takada, K., Ito, Y., and Komori, T. (2004) *Genes Dev.* **18,** 952–963
10. Boyde, A., and Shapiro, I. M. (1980) *Histochemistry* **69,** 85–94
11. Mansfield, K., Raipurohit, R., and Shapiro, I. M. (1999) *J. Cell. Physiol.* **179,** 276–286
12. Mansfield, K., Teixeira, C. C., Adams, C. S., and Shapiro, I. M. (2001) *Bone (Elmsford)* **28,** 1–8
13. Mwale, F., Tchetina, E., Wu, C. W., and Poole, A. R. (2002) *J. Bone Miner. Res.* **17,** 275–283
14. Sabbagh, Y., Carpenter, T. O., and Demay, M. B. (2005) *Proc. Natl. Acad. Sci. U. S. A.* **102,** 9637–9642
15. Nagata, S. (1997) *Cell* **88,** 355–365
16. Gross, A., McDonnell, J. M., and Korsmeyer, S. J. (1999) *Genes Dev.* **13,** 1899–1911
17. Strasser, A., O'Connor, L., and Dixit, V. M. (2000) *Annu. Rev. Biochem.* **69,** 217–245
18. Huang, D. C., and Strasser, A. (2000) *Cell* **103,** 839–842
19. Kitamura, T. (1998) *Int. J. Hematol.* **67,** 351–359